healthy but have high levels of serum GM-CSF autoantibodies. This possibility is consistent with the recent report that 31% of people with autoimmune PAP were asymptomatic.[27] Alternatively, GM-CSF autoantibodies may normally be present in healthy people but at low levels and/or in a form not detected in typical immunoassays. Other cytokine autoantibodies have been reported, although their significance remains unclear.[28,29]

We hypothesized that GM-CSF autoantibodies are ubiquitous in humans and function by scavenging and neutralizing free GM-CSF, thereby reducing nonspecific endocrine signaling and myeloid cell priming. Our experiments address the question of why high levels of GM-CSF autoantibody are virtually 100% specific and sensitive for a diagnosis of autoimmune PAP,[4,19,27,30] yet the level of autoantibody does not correlate with the severity of the disease.[31] We tested the hypothesis that GM-CSF autoantibodies rheostatically reduce myeloid cell functions and, above a critical threshold, eliminate GM-CSF signaling altogether. Results provide an estimate of this critical threshold and its association with PAP, help define the therapeutic window for potential future use of GM-CSF autoantibodies to treat inflammatory or autoimmune diseases, and describe a previously unrecognized potential mechanism of innate immune regulation.

Methods

Participants

The institutional review board of the Cincinnati Children's Hospital Medical Center approved this study. All participants or their legal guardians gave written informed consent; minors gave assent in accordance with the Declaration of Helsinki. Volunteers were enrolled into the study as healthy subjects. This group included 57 women and 15 men; mean (± SE) age was 30 plus or minus 0.63 years. All were nonsmokers, were disease-free without a history of major illness, and were symptom-free at the time of enrollment in the study. Patients with autoimmune PAP were recruited from the Rare Lung Diseases Clinic at the University of Cincinnati Medical Center, the Cincinnati Children's Hospital Medical Center, or Niigata Medical and Dental University. The diagnosis of autoimmune PAP was based on clinical and radiographic findings, an open lung biopsy, transbronchial lung biopsy, or cytologic analysis of bronchoalveolar lavage cells and fluid[4] and a positive GM-CSF autoantibody test.[5] This group included 12 women and 11 men; mean age (± SE) was 38 plus or minus 4.0. Of these, 2 (1 man, 1 woman) were in remission (defined as being asymptomatic at the time of enrollment and not requiring treatment of PAP lung disease in the preceding 5 years). All others had active PAP lung disease (defined as having symptoms typical of PAP [eg, dyspnea] and an ongoing requirement for treatment for PAP lung disease at the time of enrollment into the study).

Reagents

Phycoerythrin-conjugated anti–human CD11b antibodies (347557)[5] and fluorescein isothiocyanate–conjugated anti–human CD16 antibodies (555406)[5] were from BD Biosciences (San Jose, CA). Antibodies against STAT5 (SC-835) and actin (SC-1616) were from Santa Cruz Biotechnology (Santa Cruz, CA). Antibodies against STAT5A (71-2400) and STAT5B (71-2500) were from Zymed Laboratories (South San Francisco, CA). The phospho-STAT5 antibody (05-495) was from Millipore (Billerica, MA). Horseradish peroxidase (HRP)–conjugated goat anti–human IgG antibodies (A-2290) and rabbit anti–bovine serum albumin (BSA; B-7276)[32] were from Sigma-Aldrich (St Louis, MO). Rabbit anti–human GM-CSF polyclonal antibodies (AB-9667) were from Abcam (Cambridge, MA). Biotinylated goat anti–human GM-CSF polyclonal antibodies (BAF215) were from R&D Systems (Minneapolis, MN). Recombinant human GM-CSF was from Berlex Laboratories (Wayne, NJ; yeast-derived, glycosylated form [Leukine]), Invitrogen (Carlsbad, CA; *Escherichia coli*–derived, unglycosylated form), or PerkinElmer Life and Analytical Sciences (*E coli*–derived, ^{125}I-labeled). The GM-CSF–dependent cell line TF-1 (CRL-2003) was from ATCC. Recombinant IL-8 was from R&D Systems. Protein G columns (17-0404-01) and HiTrap NHS-activated affinity chromatography columns (17-0716-01) were from GE Healthcare (Chalfont St Giles, United Kingdom). Microcon YM-100 filters (42 424) were from Millipore. Nile red–labeled fluorescent microspheres (FP-2056-2) were from Spherotech (Lake Forest, IL). Diethylenetriamine pentaacetic acid (D6518) and ExtrAvidin HRP solution (E2886) were from Sigma-Aldrich. The RIPA Lysis Buffer Kit (24948) was from Santa Cruz Biotechnology.

Purification of GM-CSF autoantibodies

IgG was isolated from serum or commercial IVIG using protein G affinity chromatography as directed by the manufacturer. To remove bound GM-CSF, purified IgG was subjected to ultrafiltration under acidic conditions, pH 2.8, using Microcon YM-100 filters as directed by the manufacturer.[29] IgG recovered from the retentate cup in phosphate-buffered saline (PBS), pH 7.4, was further purified by GM-CSF affinity chromatography on GM-CSF–coupled NHS HiTrap columns as described previously.[5,20] In brief, purified, ultrafiltered IgG was loaded onto the GM-CSF affinity column, and the effluent and 10 mL wash buffer was collected (unbound fraction). GM-CSF–bound proteins were then eluted using 10 mL 100 mmol/L glycine-HCl (pH 2.8; bound fraction).

Far-Western blotting

Bound or unbound immunoglobulin fractions from GM-CSF affinity chromatography were fractionated by sodium dodecyl sulfate (SDS)–polyacrylamide electrophoresis (PAGE) on 2% to 15% gradient gels under nonreducing conditions (30 mA, 150 minutes). Fractionated proteins were transferred onto polyvinylidene difluoride (PVDF) membranes by electroblotting (12 volts, 75 minutes). Membranes were incubated with blocking solution (PBS containing 1% (wt/vol) BSA and 0.1% (vol/vol) Tween 20; 4°C, overnight), washed, and then incubated with ^{125}I–GM-CSF (0.16 nM, room temperature, 1 hour), washed, and subjected to autoradiography to localize bound GM-CSF.

Liquid chromatography/tandem mass spectroscopy

GM-CSF–bound proteins were fractionated by gel electrophoresis as above. The single visible bands corresponding in molecular mass to that of IgG were cut out of the gel, minced, digested with trypsin (37°C, overnight), and evaluated with Micromass Quadrupole Time-Of-Flight II mass spectrometer (Waters, Milford, MA). Results were analyzed using the Mascot search engine.[33,34] The top 50 best matching proteins for each subject were analyzed. All matches had a probability-based molecular weight search (Mowse) score over 64 that indicated a specific, nonrandom match (P value $< .05$).

ELISA

IgG subclasses. The concentration of IgG subclasses in affinity-purified GM-CSF autoantibodies was measured using a commercial enzyme-linked immunosorbent assay (ELISA [99-1000; Zymed Laboratories]).

GM-CSF autoantibody. Serum GM-CSF autoantibody levels were measured using a sandwich ELISA as described previously[5,20] with slight modifications. In brief, microtiter plates (96-well, Maxisorp; Nalge Nunc International, Rochester, NY) were coated with recombinant human GM-CSF (1 μg/mL in PBS, 4°C, overnight), washed (PBS containing 0.1% Tween 20), blocked with Stabilcoat (room temperature, 1 hour; Surmodics, Eden Prairie, MN). Serum samples were diluted 1/100 (for healthy subjects) or 1/3000 (for patients with PAP) in sample dilution buffer (PBS, 1% [wt/vol] BSA, 0.1% [vol/vol] Tween 20), and 50 μL were incubated in duplicate wells (room temperature, 40 minutes). Plates were washed and incubated with ammonium acetate (10 mM, pH 5.0, room temperature, 15 minutes) to remove nonspecific binding. Bound IgGs were detected with goat anti–human IgG-HRP diluted 1/3000 with sample dilution buffer

(room temperature, 30 minutes) and imaged with 3,3′,5,5′-tetramethylbenzidine (TMB) substrate solution (50 μL; T4444; Sigma-Aldrich) followed by addition of 1 N H_2SO_4 and read at 450 nm wavelength with Benchmark ELISA plate reader (Bio-Rad Laboratories, Hercules, CA). The accuracy and precision of the assay were determined (Table S1, available on the *Blood* website; see the Supplemental Materials link at the top of the online article).

Free GM-CSF. Serum concentrations of free GM-CSF (ie, not bound to GM-CSF autoantibody) were measured using Quantikine HS Human GM-CSF ELISA kits (R&D Systems) according to the manufacturer's instructions. The sensitivity of the assay was 0.26 pg/mL.

Total GM-CSF. Serum concentrations of total GM-CSF (ie, autoantibody-bound plus free GM-CSF) were measured using a novel sandwich ELISA based on a method developed for measurement of HIV-1 p24 antigen.[35] Microtiter plates were coated with capture antibody (PBS containing 1 μg/mL rabbit anti–human GM-CSF antibody, 4°C, overnight), and blocked with PBS containing 1% (wt/vol) BSA. To evaluate the detection of free GM-CSF and autoantibody-bound GM-CSF in serum, a set of standard samples composed of recombinant human GM-CSF (Leukine) ranging from 0 to 30 ng/mL was prepared in mouse serum in the absence or presence of purified human GM-CSF autoantibodies (30 μg/mL). Aliquots (10 μL) of serum or standard control samples were mixed with 20 μL pretreatment buffer (SDS-HD buffer; PBS, 1% SDS, 1.5 mM diethylenetriamine pentaacetic acid, pH 7.4, and incubated (95°C, 5 minutes). After chilling briefly on ice, 270 μL PBS containing 1% (wt/vol) BSA was added to quench residual SDS. Duplicate aliquots (50 μL) of samples were applied to wells, and the plates were incubated (room temperature, 90 minutes), washed, and then incubated with detection antibody solution (PBS containing 1% [wt/vol] BSA, 500 ng/mL biotin-conjugated goat anti–human GM-CSF antibody; room temperature, 90 minutes). Detection was enhanced by incubation with ExtrAvidin HRP solution (diluted 1/250; room temperature, 30 minutes), imaged by TMB solution followed by addition of 1 N H_2SO_4 and read at a wavelength of 450 nm with Benchmark ELISA plate reader.

Phospho-STAT5 immunoblotting

Neutrophils were isolated on Ficoll gradients, followed by red blood cell lysis. More than 97% of the isolated cells consist of granulocytes. Isolated neutrophils were resuspended (5×10^6 cells/mL) in assay buffer (Hank balanced salt solution [HBSS] containing 10% fetal bovine serum, 25 mmol/L HEPES, pH 7.4) and incubated with various concentrations of purified GM-CSF autoantibodies (0, 0.01, 0.1, 0.5, 1.0 μg/mL) and GM-CSF (Leukine, 10 ng/mL) for 15 minutes at 37°C. After incubation, cells were collected by centrifugation, washed with PBS, and suspended in 200 μL RIPA buffer, which consisted of 0.05 mol/L Tris-HCl, pH 8.0, 0.15 M NaCl (Tris-buffered saline [TBS]), 1% [vol/vol] Nonidet P-40, 0.5% [wt/vol] sodium deoxycholate, 0.1% [wt/vol] SDS, 0.004% [wt/vol] sodium azide) containing 2% (vol/vol) proteinase inhibitor cocktail, phenylmethylsulfonyl fluoride, and sodium orthovanadate as directed by the manufacturer. Samples were kept on ice for 30 minutes, and soluble lysate was collected after removing insoluble debris (9000*g*, 4°C, 15 minutes). Neutrophil lysate was then fractionated on SDS-PAGE gels (4%-12% Tris Glycine Gel; Invitrogen) and transferred to PVDF membranes by electroblotting. After blocking the membrane with TBS, 5% [wt/vol] dry milk, 0.1% [vol/vol] Tween 20 (4°C, overnight), phosphorylated-STAT5 was detected with murine anti–phospho-STAT5 antibody (diluted 1/500) followed by the incubation with HRP-conjugated sheep anti–murine IgG and imaged with ECL-Plus (GE Healthcare) as directed by the manufacturer. This procedure was used for measuring STAT5A, STAT5B, total STAT5, and actin in the same samples with the appropriate antibodies. Band intensity was quantified using KODAK Image Station 440FC equipped with KODAK 1D Image Analysis Software (Carestream Health, Rochester, NY), and the ratio of phosphorylated STAT5 to total STAT5 was calculated.

Serum GM-CSF–neutralizing capacity (TF-1 cell) assay

GM-CSF neutralization activity was evaluated using the GM-CSF–dependent cell line, TF-1 as described previously.[20] In brief, cells were cultured in the absence or presence of GM-CSF autoantibodies purified from equal volumes (30 μL) of serum or IVIG (600 μg/well). After 4 days in culture, cell proliferation was measured using the TACS 3-(4,5-dimethylthiazol-2-yl)-2,5-diphenyltetrazolium assay kit (R&D Systems) according to the manufacturer's instructions.

Neutrophil CD11b stimulation index assay

The neutrophil stimulation assay was performed as described previously.[5] In brief, aliquots of heparinized fresh whole blood were incubated with GM-CSF, and then cell-surface CD11b levels were quantified by flow cytometry. The CD11b stimulation index is calculated as the mean fluorescent intensity of stimulated neutrophils minus the mean fluorescent intensity of unstimulated neutrophils divided by mean fluorescent intensity of unstimulated neutrophils and multiplied by 100.

Neutrophil chemotaxis assay

Neutrophils were isolated as above and suspended (4×10^6 cells/mL) in HBSS supplemented with 0.1% (wt/vol) BSA, 1 mM $CaCl_2$, and 1 mM $MgCl_2$ with or without various doses of GM-CSF autoantibodies. Neutrophil chemotactic capacity was evaluated using Transwell (Corning Life Sciences, Acton, MA) with 3-μm pore size with 10 ng/mL rhIL-8 as a chemoattractant. One hundred microliters of cell suspension was transferred to upper chamber and incubated for 2 hours at 37°C, 5% CO_2. After incubation, neutrophils migrating into the lower chamber were enumerated using a hemocytometer.

Neutrophil phagocytosis assay

The phagocytic capacity of neutrophils in whole blood (hereafter called the phagocytic capacity) was measured by flow cytometry as described previously.[5] In brief, triplicate samples of heparinized human blood were incubated with IgG-opsonized fluorescent microspheres[32] with gentle orbital rotation. Uptake of microspheres by neutrophils was evaluated with flow cytometry. Phagocytic capacity was calculated as the percentage of neutrophils containing internalized microspheres multiplied by the mean fluorescence intensity of phagocytic neutrophils and multiplied by the neutrophil count in blood. This assay was validated using isolated neutrophils (Figure S2).

Alveolar macrophage phagocytosis assay

Human alveolar macrophages were obtained from lung bronchoalveolar or whole lung lavage fluid and then washed, resuspended, and seeded into 35-mm culture dishes as described previously.[1] Cells were incubated with heat-killed *E coli*, *Staphylococcus aureus*, zymosan, or 0.1-μm latex beads, each fluorescently labeled with Texas Red (Invitrogen), fixed and examined by fluorescence microscopy[36] as described previously[1] to evaluate alveolar macrophage phagocytosis.

Statistical analysis

Numerical data were evaluated for a normal distribution using the Kolmogorov-Smirnov test and for equal variance using the Levene median test; parametric data are presented as means (± SE), and nonparametric data are presented as medians and interquartile ranges. Categorical data are presented as a percentage of the total or numerically, as appropriate. Statistical comparisons of parametric data were made with the Student *t* test for 2-group comparisons and with Kruskal-Wallis one-way analysis of variance with post-hoc analysis according to the Holm-Sidak method for multiple-group comparisons. Nonparametric data were compared with the use of the Kruskal-Wallis rank-sum test. Correlation coefficients were obtained using the Spearman correlation method. All tests were 2-sided, and *P* values of less than .05 were considered to indicate statistical significance. Regression analysis was performed with Spearman rank order correlation

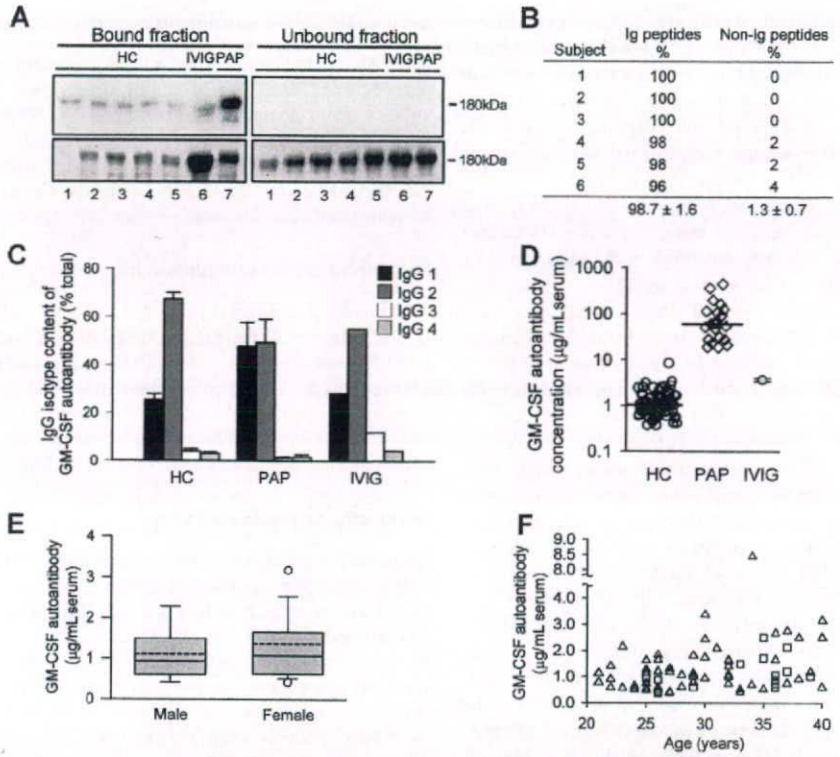

Figure 1. Presence of GM-CSF autoantibodies in healthy subjects. (A) Total IgG was isolated from the serum of healthy control subjects (HC) or patients with PAP (PAP) or from pharmaceutical grade IVIG by protein G chromatography and subjected to ultrafiltration under acidic conditions to remove bound GM-CSF. GM-CSF autoantibodies were then isolated by GM-CSF affinity chromatography and evaluated by far-Western analysis probed with ^{125}I-GM-CSF. Shown are Coomassie Blue–stained electrophoresis gels (bottom panels) and corresponding far-Western blots (top panels). Each numbered lane represents the corresponding bound (left panels) and unbound (right panels) chromatography fractions from 1 subject or sample. (B) Serum GM-CSF–binding proteins from 6 healthy human subjects were fractionated individually on gels as in panel A, and proteins in the 180-kDa band from each were extracted, subjected to liquid chromatography and tandem mass spectroscopy, and the results evaluated by comparison to Mascot database as described under "Methods." Only matches with a probability-based Mowse score greater than 64 (indicating a P value < .05) were considered in the analysis. The percentages of immunoglobulin (Ig) and non-Ig peptides among the top 50 peptide fragment matches identified for each sample are shown. (C) GM-CSF autoantibodies were isolated by GM-CSF affinity chromatography from serum of healthy subjects (HC; n = 10), patients with PAP (PAP, n = 4), or from pharmaceutical IVIG (n = 1 clinical grade vial), and the percentage of IgG subtypes was measured by ELISA. (D) Serum GM-CSF autoantibody concentrations in healthy subjects (HC), patients with PAP (PAP), or IVIG (reconstituted at 9.94 mg/mL in PBS). Serum GM-CSF autoantibody levels in healthy subjects (median (interquartile range [IQR]) = 1.04 [0.63-1.7] µg/mL, n = 72) were lower than in patients with PAP (median [IQR] = 59.8 (27.4–116.5) µg/mL; n = 21; P < .001). Median values (HC, PAP) are indicated by a horizontal bar. (E) Serum GM-CSF autoantibody levels in males (n = 15) and females (n = 57). Data are shown as whisker plots indicating the interquartile range (upper and lower borders of box), the 90th and 10th percentile (error bars), the 95th and 5th percentile (upper and lower open symbols), the median (solid horizontal line in box), and mean (dashed line in box) values of GM-CSF autoantibody levels. (F) Serum GM-CSF autoantibody levels in healthy women (△) and men (□) of various ages (n = 72). Regression analysis did not reveal a significant correlation GM-CSF autoantibody levels with age (R^2 = 0.08).

using SigmaPlot software (version 8.0; Systat Software, San Jose, CA). All experiments were repeated at least twice, with similar results.

Results

Circulating GM-CSF autoantibodies in healthy subjects

To determine whether GM-CSF autoantibodies are normally present in healthy persons, we used a novel method[29] based on the prior removal of potentially bound GM-CSF. GM-CSF-binding immunoglobulins similar in molecular weight to IgG were detected in all healthy subjects evaluated, in pharmaceutical IVIG, and in a patient with PAP (as a positive control; Figure 1A). Liquid chromatography and tandem mass spectroscopy confirmed the authenticity of the autoantibodies in healthy subjects, demonstrating they were composed exclusively of immunoglobulin (Figure 1B). IgG subtyping further demonstrated they were composed primarily of IgG1 and IgG2 with only small amounts of IgG3 and IgG4 and had a similar composition in healthy persons, patients with PAP, and IVIG (Figure 1C). Using a sensitive and specific ELISA (Figure S1A-C), GM-CSF autoantibodies were detected in all samples evaluated, including the serum from 72 healthy persons, 21 patients with PAP, and IVIG (Figure 1D). The serum concentration of GM-CSF autoantibodies in healthy subjects was similar to that of pharmaceutical IVIG reconstituted at physiologic serum IgG concentration and was markedly lower than serum levels in patients with PAP (Figure 1D). GM-CSF autoantibody levels in healthy subjects were unaffected by sex (Figure 1E) or age (Figure 1F). These results demonstrate that GM-CSF autoantibodies are common or ubiquitous in healthy persons, albeit at levels far lower than in patients with PAP.

Circulating complexes of autoantibody and GM-CSF

To determine whether GM-CSF was bound to circulating GM-CSF autoantibodies, potentially interfering with detection, total serum IgG was isolated on protein G, washed to remove proteins not directly bound to autoantibodies, eluted, and evaluated by Western blotting. GM-CSF bound to IgG was present in all healthy subjects and in patients with PAP evaluated, thus demonstrating the presence of GM-CSF-autoantibody complexes (Figure 2A). To determine whether immune complex formation interfered with detection of serum GM-CSF, we first measured the concentration of GM-CSF in the absence or presence of GM-CSF autoantibodies. GM-CSF autoantibodies completely abolished detection of GM-CSF using a commercially available ELISA

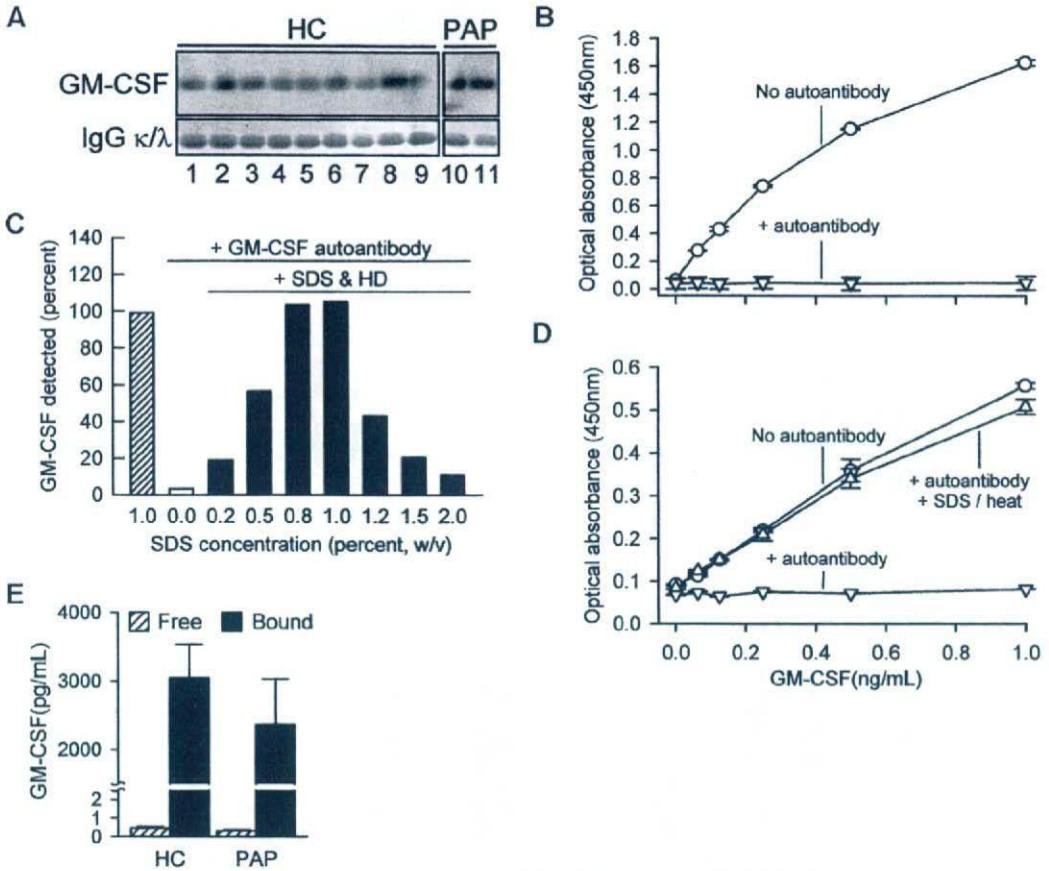

Figure 2. Concentration of free and IgG-bound GM-CSF in human serum. (A) Total IgG was isolated individually from the sera of healthy subjects (HC) or patients with PAP (PAP) using protein G and evaluated by Western blotting to detect GM-CSF (top panels) or IgGκ (κ) and -λ (λ) light chains (as a loading control, bottom blots). Each lane represents one subject. (B) Detection of free GM-CSF and autoantibody-bound GM-CSF in serum. A set of "standard" samples composed of recombinant human GM-CSF (Leukine) at various concentrations ranging from 0 to 30 ng/mL were prepared in mouse serum in the absence (○) or presence (▽) of purified human GM-CSF autoantibodies (30 μg/mL). Standard samples were diluted 1/30 with 1% BSA in PBS and then GM-CSF was measured using a commercial human ELISA kit (R&D Systems) as directed by the manufacturer. (C) Use of a novel ELISA (SDS-HD ELISA, see "Methods") to quantify GM-CSF in PBS in the absence or presence of GM-CSF autoantibody (1 μg/mL) and in the absence or presence of a pretreatment with SDS and heat denaturation. Each bar represents the mean of duplicate determinations for 1 of 4 separate experiments with similar results. (D) GM-CSF level evaluated using a novel human GM-CSF ELISA as described in "Methods." Symbols represent the same samples and conditions as described in the legend to panel B above. GM-CSF was detectable in the absence of GM-CSF autoantibody (○), undetectable in the presence of GM-CSF autoantibody in the absence of SDS-HD pretreatment (▽), and detection was restored in the presence of GM-CSF autoantibody by SDS-HD pretreatment (△). (E) Free GM-CSF (▨) or total GM-CSF (free and autoantibody-bound; ■) were measured in sera of healthy subjects (HC) or patients with PAP (PAP) using a commercially available ELISA or the SDS-HD ELISA, respectively, as described in "Methods." Total serum GM-CSF levels in HC and PAP were not different (3048 ± 484, n = 11; PAP 2360 ± 668, n = 5; respectively, $P = .43$).

(Figure 2B). We then developed a novel ELISA using a polyclonal capture antibody and pretreatment with SDS and heat denaturation that enabled detection of both free GM-CSF and GM-CSF bound to autoantibody (Figure 2C,D). Using this ELISA, the mean (± SE) total serum GM-CSF concentration in healthy subjects was 3047 plus or minus 484 pg/mL (Figure 2E). Similar levels of total serum GM-CSF levels were observed in patients with PAP. In contrast, levels of free GM-CSF measured using the commercial ELISA (see Figure 2B) were less than 1 pg/mL in both groups (Figure 2E). Thus, serum GM-CSF was more abundant than previously reported[12,13] and existed almost exclusively in a form complexed to IgG in health and disease with less than 0.1% present in the unbound form.

Effects of circulating GM-CSF autoantibodies on GM-CSF signaling

To determine the significance of GM-CSF autoantibodies in healthy subjects, we evaluated their effects on GM-CSF signaling. Using a bioassay based on GM-CSF–dependent proliferation of TF-1 cells,[20] autoantibody-dependent GM-CSF–neutralizing activity was detected in IgG isolated from all persons evaluated, and levels fell between that of serum from a patient with PAP as a positive control and culture media as a negative control (Figure 3A). IVIG reconstituted at physiologic IgG concentration also contained GM-CSF–neutralizing activity at levels similar to serum from healthy subjects. GM-CSF autoantibodies reduced GM-CSF signaling in a concentration-dependent fashion as shown by the decrease in GM-CSF–stimulated phosphorylation of signal transducer activation and transcription 5 (STAT5), a downstream signaling molecule (Figure 3B). Although low concentrations of free GM-CSF were highly bioactive, 5-fold higher concentrations of autoantibody-bound GM-CSF had practically no signaling activity (Figure 3C). GM-CSF stimulates increased levels of CD11b on neutrophils, a phenomenon we previously exploited in developing an assay to measure GM-CSF–neutralizing activity in whole blood.[5] Low concentrations of GM-CSF–stimulated maximal CD11b levels in healthy persons but had no effect in patients with PAP (Figure 3D). The block in stimulation of CD11b levels caused by higher GM-CSF autoantibody levels in patients with PAP could be overcome by exposure to high concentrations of GM-CSF (Figure 3D inset). Highly purified GM-CSF autoantibodies

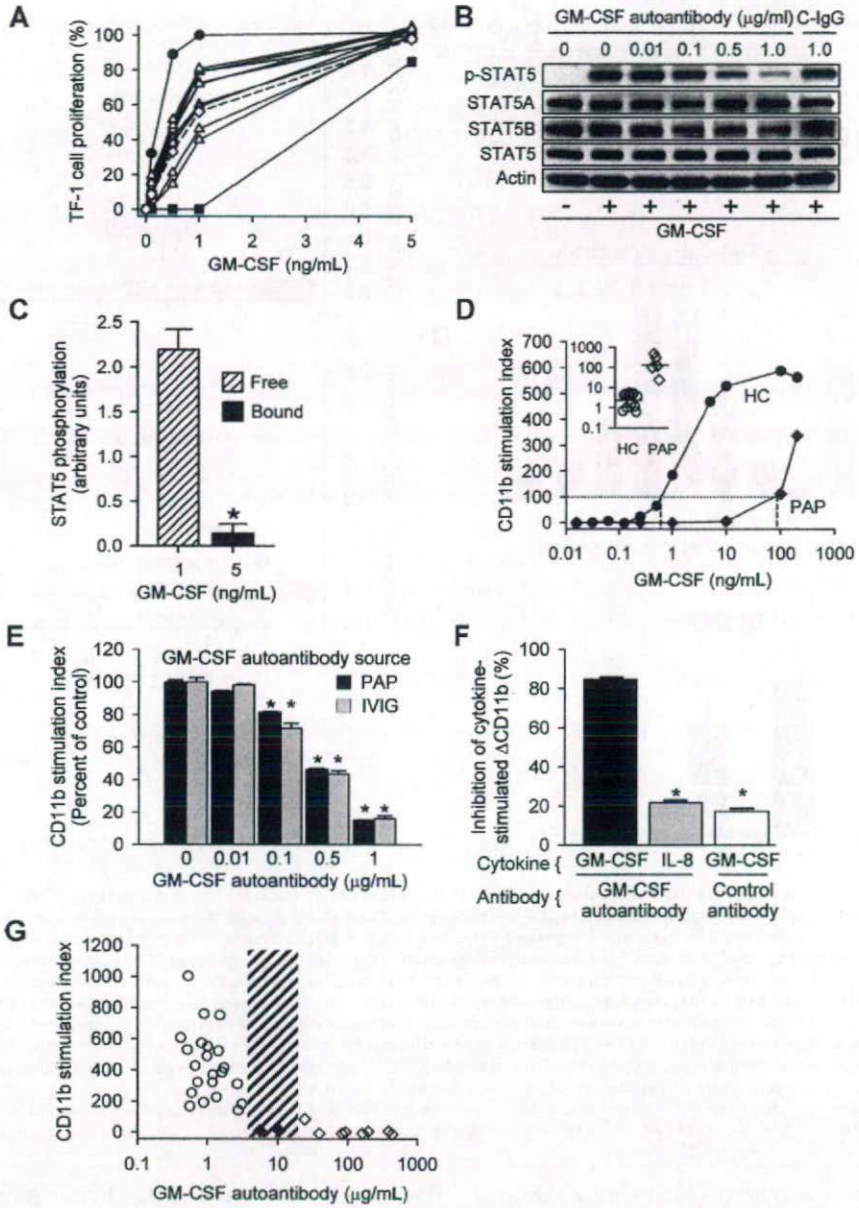

Figure 3. Regulation of GM-CSF signaling by GM-CSF autoantibodies in healthy subjects and patients with PAP. (A) The serum GM-CSF–neutralizing capacity of GM-CSF autoantibodies was measured using the TF-1 cell-proliferation assay.[20] Equal volumes (30 μL) of serum from healthy subjects (△) or a PAP patient (■) (as a positive control), IVIG reconstituted at physiologic concentration (◇), or culture media (●) (as a negative control) were evaluated. The neutralizing capacity of purified GM-CSF autoantibodies from HC serum or IVIG (dashed line) was intermediate between that of autoantibodies isolated from serum the patient with PAP, which contains high concentrations of GM-CSF autoantibody, and control media, which contains none. (B) Neutrophils isolated from healthy subjects were incubated with various concentrations of GM-CSF affinity-purified autoantibodies isolated from IVIG or with control antibody (1 μg/mL) and stimulated with 10 ng/mL GM-CSF for 15 minutes and total and phosphorylated STAT5 (pSTAT5) was measured by immunoblotting. (C) The signaling activity of free and autoantibody-bound GM-CSF was measured by quantifying the level of STAT5 phosphorylation in isolated neutrophils by immunoblotting (shown as the ratio of phosphorylated STAT5 to total STAT5) as described in "Methods." The signaling activity of GM-CSF complexed to autoantibody was markedly lower than free GM-CSF (0.142 ± 0.1 vs 2.192 ± 0.2 pg/mL, respectively; n = 3 each; $^*P < .001$). (D) The typical pattern of GM-CSF–stimulated increase in CD11b levels on neutrophils in whole blood (CD11b stimulation index) is shown for a healthy subject (HC) and a patient with PAP (PAP). The amount of exogenous GM-CSF (dashed lines) required to stimulate an increase in neutrophil CD11b levels to the threshold value (dotted line) was lower in HCs than in patients with PAP. The median (IQR) GM-CSF concentration required to reach this stimulation threshold (inset) was significantly higher in patients with PAP than in healthy subjects (120 [80-347] ng/mL, n = 5; and 3.96 [1.07-4.86] ng/mL; n = 12; respectively; $P < .002$, Mann-Whitney). (E) Concentration-dependent reduction in the CD11b stimulation index by GM-CSF autoantibody purified from IVIG (□) or patients with PAP (■) and incubated with fresh whole blood at various concentrations. Each bar represents the results of 3 separate determinations. *Significant decrease ($P < .001$) from baseline determined in the absence of GM-CSF autoantibody. (F) Specificity of purified GM-CSF autoantibody. Neutrophils were incubated in the presence of GM-CSF (10 ng/mL) or IL-8 (100 ng/mL) and in the absence or presence of 1 μg GM-CSF autoantibody or control IgG as indicated. Data represent the level of CD11b in stimulated cells—the level in unstimulated cells. GM-CSF autoantibodies markedly inhibited the GM-CSF–stimulated (■), but resulted in levels of inhibition by IL-8 (□) that were significantly lower and similar to control (IgG, □). *A significant difference ($P < .001$) compared with inhibition of the GM-CSF–stimulated increase by GM-CSF autoantibody (■). (G) The CD11b stimulation index was measured in fresh blood from healthy control subjects (○), patients with PAP with active disease (◇), or patients with PAP in clinical remission of the lung disease (◆). The range of serum GM-CSF autoantibody levels separating healthy subjects and patients with PAP with active disease evaluated with this assay is indicated (3.2-24 μg/mL, ▨). Each symbol represents the results of triplicate determinations for one subject. The median (IQR) free serum GM-CSF level in healthy subjects was 0.00 (0.00-0.390) pg/mL and did not correlate with the CD11b stimulation index ($P > .05$), whereas the median (IQR) GM-CSF autoantibody level (0.90 [0.58-1.19] μg/mL) correlated with CD11b stimulation index ($R^2 = 0.46$, $P = .03$) (Spearman rank order correlation).

isolated from IVIG or patients with PAP blocked the increase in CD11b levels to a similar degree and in a concentration-dependent fashion (Figure 3E). Purified GM-CSF autoantibodies were specific and did not block an IL-8–stimulated increase in CD11b levels (Figure 3F). To determine the endogenous autoantibody level associated with complete loss of GM-CSF signaling in vivo, the CD11b stimulation index was measured in whole blood from healthy subjects and patients with PAP. The CD11b stimulation index correlated inversely with endogenous levels of serum GM-CSF autoantibody up to 5.7 μg/mL and was zero over a wide range of higher concentrations (Figure 3G). It is noteworthy that all positive results below this autoantibody level (referred to as the critical threshold for CD11b stimulation) were from healthy subjects and all negative results above it were from patients with PAP. Thus, GM-CSF autoantibodies seem to scavenge free GM-CSF in vivo and modulate the endocrine signaling capacity of GM-CSF in whole blood, suggesting that they may function to negatively regulate GM-CSF signaling in health and disease.

Effects of circulating GM-CSF autoantibodies on myeloid cell functions

The functional significance of GM-CSF autoantibodies in healthy subjects was evaluated by correlating levels with endogenous neutrophil functions. We recently developed a method to measure neutrophil phagocytosis in whole blood and then showed that transfer of GM-CSF autoantibodies into healthy human blood reduced neutrophil phagocytosis in a concentration-dependent fashion.[5] Here, we verified that the assay can detect differences in the baseline phagocytic capacity of neutrophils among healthy subjects (Figure S2) and then measured the endogenous, phagocytic capacity of unstimulated neutrophils in whole blood from healthy subjects and patients with PAP. Neutrophil phagocytic capacity decreased with increasing endogenous GM-CSF autoantibody levels up to 3.2 μg/mL in healthy persons and reached a trough level and was unchanging over a wide range of higher concentrations above 39 μg/mL in patients with active PAP (Figure 4A). Two patients in remission of PAP lung disease who had lower serum GM-CSF autoantibody levels (5.7 and 10.4 μg/mL) had a neutrophil phagocytic capacity in the normal range, indicating the critical threshold of serum GM-CSF autoantibodies associated with reduced neutrophil phagocytosis might lie between 10.4 and 39 μg/mL. GM-CSF autoantibodies, at levels similar to those present in healthy subjects, reduced interleukin 8–stimulated neutrophil chemotaxis in vitro in a concentration-dependent fashion by a mechanism not attributable to chemokinesis or nonspecific effects (Figure 4B). Together, these results suggest that the low levels of GM-CSF autoantibodies present in healthy subjects may regulate GM-CSF–dependent neutrophil functions rheostatically and that the critical threshold level of GM-CSF autoantibodies associated with loss of GM-CSF priming of neutrophil functions in patients with PAP is between 10.4 and 39 μg/mL.

Because GM-CSF deficiency in mice impairs alveolar macrophage functions, including phagocytosis of *E coli*, *S aureus*, *Mycobacterium tuberculosis*, yeast particles (zymosan), and latex beads,[1,32,37,38] we evaluated phagocytic function of alveolar macrophages from healthy subjects and patients with autoimmune PAP. Compared with alveolar macrophages from healthy subjects, alveolar macrophages from patients with PAP had impaired phagocytosis of *E coli*, *S aureus*, zymosan, and latex beads (Figure S3) and impaired clearance of surfactant (not shown). Although high levels of GM-CSF autoantibodies are thought to cause lung disease in PAP by blocking the paracrine stimulation of alveolar

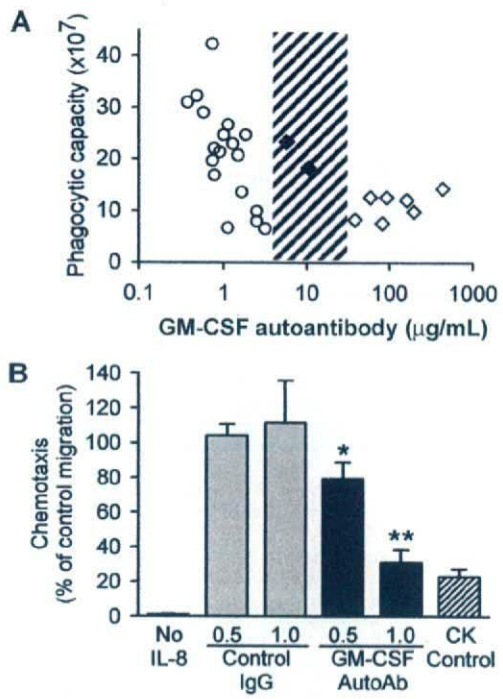

Figure 4. Correlation of GM-CSF autoantibody level and basal neutrophil function in vivo, and effects of GM-CSF autoantibody level on neutrophil function in vitro. (A) The phagocytic capacity of unstimulated neutrophils in whole blood was measured in healthy subjects (○), patients with PAP with active disease (◇), and patients with PAP in clinical remission of the lung disease (◆) by quantifying the uptake of IgG-opsonized latex microspheres as described under "Methods." The range of serum GM-CSF autoantibody levels separating healthy subjects and patients with PAP with active disease evaluated with this assay is indicated (3.2-39 μg /mL, ▨). Each symbol represents the results for triplicate determinations for one subject. The mean (IQR) free serum GM-CSF in healthy subjects was 0.00 (0.00-0.267) pg/mL serum and did not correlate with the neutrophil phagocytic capacity ($P > .05$), whereas GM-CSF autoantibody levels (1.07 [0.74-1.66] μg/mL) correlated with neutrophil phagocytic capacity ($R^2 = -0.70$, $P = .001$) (Spearman rank order correlation). (B) Neutrophil chemotaxis was measured as described in "Methods." In brief, neutrophils were placed in the upper chamber of a transwell culture plate and IL-8 (10 ng/mL) was placed in the lower chamber, both the upper and lower chambers (chemokinesis [CK] control) or was omitted (No IL-8) and GM-CSF autoantibody (0.5, or 1.0 μg/mL) or isotype control antibody (0.5 or 1.0 μg/mL) was placed in the upper chamber. Each bar represents the mean (± SE) for results from 3 determinations. Compared with the respective isotype antibody controls, increasing concentrations of GM-CSF autoantibody reduced neutrophil chemotaxis in rheostatic fashion (*$P < .05$; **$P < .005$).

macrophages by GM-CSF secreted from adjacent respiratory epithelial cells,[4,19,39] the level of GM-CSF autoantibodies associated with development of lung disease is unknown. Therefore, we measured serum GM-CSF autoantibody concentrations in healthy persons and in patients with active PAP lung disease. The critical threshold of serum GM-CSF autoantibodies associated with active PAP lung disease was between 8.5 and 19 μg/mL (Figure 5). It is noteworthy that 2 patients in remission of PAP lung disease at the time of evaluation had serum GM-CSF autoantibody levels of 5.7 and 10.4 μg/mL. Thus, the minimum serum level of GM-CSF autoantibodies associated with the presence of active lung disease in PAP lies between 10.4 and 19 μg/mL.

Discussion

Here, we demonstrate that GM-CSF autoantibodies are normally present in healthy human subjects, albeit at levels lower than in

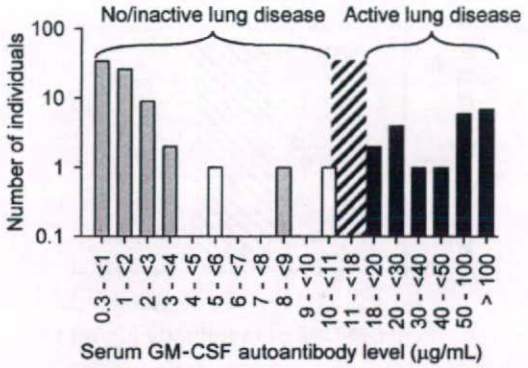

Figure 5. Histogram showing the frequency distribution of serum GM-CSF autoantibody levels in healthy subjects (□, n = 72), patients with PAP with active lung disease (■, n = 21), and patients with PAP in clinical remission of the lung disease (□, n = 2). Clinical remission was defined as formerly diagnosed patients with PAP who were currently presenting no respiratory insufficiency and had normal chest X-ray images. The range of serum GM-CSF autoantibody levels separating subjects with no or active lung disease from those without active disease is indicated (10.4-19 μg/mL, ▨).

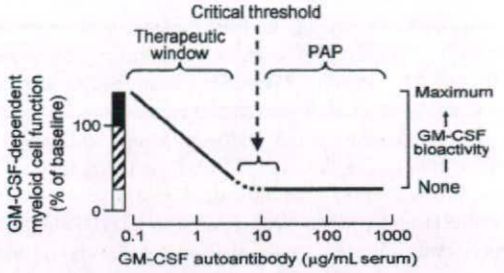

Figure 6. Schematic of the proposed mechanism of innate immune regulation by GM-CSF autoantibodies showing the relationship between endogenous GM-CSF autoantibody level (abscissa), GM-CSF–dependent myeloid cell functions, and GM-CSF bioactivity (ordinate). More than a range of low autoantibody levels present in healthy subjects, myeloid cell functions vary inversely with level of GM-CSF autoantibodies (ordinate, ▨) and increased levels of GM-CSF (eg, present at inflammatory sites or from exogenous administration) increase myeloid cell functions above baseline levels by a mechanism known as "GM-CSF priming" (ordinate, ■). At and above GM-CSF autoantibody levels sufficient to completely neutralize GM-CSF bioactivity (eg, the critical threshold), GM-CSF–stimulated myeloid cell functions are minimal or zero (ordinate, □) and the risk of PAP is increased.

patients with PAP. GM-CSF autoantibody levels correlated inversely with neutrophil functions in vivo and reduced neutrophil functions rheostatically in vitro. GM-CSF was far more abundant in healthy human serum than previously reported[12,13]; however, more than 99% was bound and inactivated by GM-CSF autoantibodies. Although the majority of serum GM-CSF was undetectable with a commercial ELISA kit, it was readily detected with a novel ELISA developed to measure both free and autoantibody-bound GM-CSF. We measured the critical threshold of GM-CSF autoantibodies associated with the presence of PAP. We conclude that GM-CSF autoantibodies scavenge free GM-CSF in vivo and may negatively modulate myeloid cell functions in health and disease.

The observation that GM-CSF autoantibodies are ubiquitous in healthy subjects has implications for the pathogenesis of PAP, suggesting it is caused by a pathologic increase in the level of preexisting GM-CSF autoantibodies rather than a new adaptive antibody response. This is supported by several findings, including that: (1) low levels of GM-CSF autoantibodies were present in all healthy persons evaluated, were inversely correlated with the CD11b stimulation index and basal neutrophil phagocytic function in vivo, and reduced the CD11b stimulation index and neutrophil chemotaxis in vitro; (2) GM-CSF autoantibodies from healthy subjects (from IVIG) and from patients with PAP reduced GM-CSF signaling in vitro to a similar degree; (3) at levels above a critical threshold, GM-CSF autoantibodies were associated with multiple simultaneously impaired GM-CSF–dependent myeloid functions; (4) GM-CSF autoantibodies were specific; (5) other anti-cytokine or noncytokine autoantibodies have not been reported in patients with PAP[20]; and (6) PAP does not occur as a complication of other more common autoimmune diseases.[27,40] Our experimental measurement of the critical threshold of GM-CSF autoantibodies associated with the presence of PAP lung disease showed it lies between 10.4 and 19 μg/mL. This agrees well with our prior estimate of 8-22 μg/mL[26] calculated from data for 1258 healthy subjects,[25] 425 patients with autoimmune diseases but without PAP,[40] and 158 patients with autoimmune PAP.[4] GM-CSF autoantibodies were distinct from the recently identified soluble GM-CSF receptor,[41] which differs in molecular weight and was not detected by far-Western blotting or by liquid chromatography and mass spectroscopy of the GM-CSF-binding band seen in the serum of healthy subjects or patients with PAP. Our study does not rule out that GM-CSF autoantibodies in healthy subjects and patients with PAP may differ in ways important to PAP pathogenesis. Examples of such potential differences include the GM-CSF epitopes targeted, the binding affinity of GM-CSF autoantibodies,[20] or the relative composition of neutralizing and non-neutralizing GM-CSF autoantibodies in healthy subjects and patients with PAP. Future studies focused on these questions and the mechanism of immune dysregulation responsible for increasing the GM-CSF autoantibody level in autoimmune PAP will be important in furthering our understanding of its pathogenesis.

These results predict a novel mechanism of innate immune regulation (Figure 6). In healthy persons, low levels of endogenous GM-CSF autoantibodies determine the ambient level of GM-CSF bioactivity, which determines the basal level of myeloid cell functions. Endogenous myeloid cell priming varies inversely with autoantibody concentration up to the critical threshold. Myeloid cell functions likely regulated by this mechanism include: surfactant catabolism, cell adhesion, phagocytosis, microbial killing, pathogen receptor expression, Toll-like receptor 4 signaling, and others.[1,5] In patients with PAP, very high levels of GM-CSF autoantibodies reduce GM-CSF bioactivity to zero,[20] thereby eliminating GM-CSF priming of myeloid cell functions. This model is consistent with reports that administration of exogenous GM-CSF antibody rheostatically reduces myeloid cell functions in vivo in mice[42] and ex vivo in human blood.[5] It is also consistent with the observation that GM-CSF bioactivity is undetectable in patients with PAP.[20] Because surfactant clearance by alveolar macrophages requires GM-CSF and GM-CSF bioactivity is eliminated at all autoantibody concentrations above the critical threshold, this model explains the lack of correlation between the level of GM-CSF autoantibody and the severity of lung disease in patients with PAP.[31] It also supports the interesting hypothesis of Bendtzen and colleagues (Svenson et al,[25] Ross et al,[43] and Metcalf et al[44]), who first proposed that the therapeutic effects of IVIG may be due to GM-CSF autoantibodies that may function by reducing GM-CSF stimulated myeloid cell reactivity.

Although multiple lines of evidence support the conclusion that GM-CSF autoantibodies are present in healthy subjects, their potential role in immune regulation is less certain. Our current and reported observations strongly support a role for GM-CSF in the constitutive regulation of myeloid cell functions in vivo and suggest that GM-CSF autoantibodies may be

important in negatively modulating GM-CSF signaling in health and disease.[1-4,20,23,24,26] The virtually complete binding and neutralization of GM-CSF suggests that GM-CSF autoantibodies may function to scavenge and inactivate GM-CSF released at sites of inflammation, thus preventing detrimental distal endocrine effects. This is consistent with the rapid, receptor-mediated clearance of GM-CSF reported in mice[45] and also with the low levels of free GM-CSF present in human serum.[5,13] Alternatively, GM-CSF present in the form of inactive circulating immune complexes may be released at sites of infection (perhaps by a drop in pH), where it could stimulate myeloid functions by locking the GM-CSF receptor into its high STAT5-mediated signaling state,[12] thereby amplifying local innate immunity on a microscopic scale. This is consistent with the observation that anti-cytokine antibody binding prolongs the half-life of interleukin-4 in vivo.[46]

Several observations have identified GM-CSF as a molecular target for therapeutic development,[22,23,47-49] including the failure of GM-CSF knockout mice to develop the typical lesions of arthritis or multiple sclerosis in experimental models of these diseases as well as the pathogenic implications of increased local levels of GM-CSF at sites of disease in rheumatoid arthritis. Administration of GM-CSF autoantibody at doses below the critical threshold may rheostatically reduce myeloid cell activity,[5,42] potentially reducing the severity of inflammatory and autoimmune disorders.[24] However, doses exceeding the critical threshold may result in excessive myeloid cell suppression and unwanted clinical manifestations, including alveolar proteinosis and impaired antimicrobial host defenses. Thus, our estimate of the critical threshold helps to define the therapeutic window for the safe use of GM-CSF autoantibodies in potential new clinical therapies. The close agreement of estimates based on various myeloid functions suggests that serum GM-CSF autoantibody levels below 10 μg/mL may not result in adverse clinical manifestations. However, it is also possible that different critical threshold values may exist for distinct GM-CSF–regulated myeloid cell functions (eg, surfactant catabolism, antimicrobial host defense functions), different modes of GM-CSF signaling (eg, endocrine, autocrine, and paracrine), or various tissue compartments (eg, lung versus blood). For example, a lower concentration of GM-CSF is required for maintenance of alveolar macrophage-mediated surfactant clearance than for normal alveolar macrophage immune functions (B.C.C. and B.C.T., unpublished observations). Separately, it is possible that clinically safe levels of very highly purified GM-CSF autoantibodies may be lower than levels predicted from data based on endogenous autoantibody levels because autoantibody potency is increased by removal of GM-CSF. This is consistent with the observation that estimates of the critical threshold obtained by correlating levels of endogenous GM-CSF autoantibody and neutrophil functions in unstimulated whole blood (Figures 3G and 4A) are higher than estimates from experiments in which highly purified GM-CSF autoantibodies are incubated with healthy human blood.[5] It is important to note that GM-CSF autoantibody levels are relative values linked to the autoantibody standard used in their measurement. Thus, standardization of these methods will be useful to ensure comparability of future studies.

Acknowledgments

We thank Jonathan Puchalski, John Howington, and Michael Reed (University of Cincinnati Medical Center, Cincinnati, OH) for help with the care of patients with PAP and clinical sample collection, and Drs. Jeffrey Whitsett, Fred Finkelman, and Christopher Karp (Cincinnati Children's Hospital Medical Center, Cincinnati, OH) for their critical reading of the manuscript.

This work was supported by the National Institutes of Health (Bethesda, MD; HL085453 to B.C.T.), National Center for Research Resources (Bethesda, MD; RR019498 to B.C.T.), and the Japan Society for the Promotion of Science (Tokyo, Japan; B19390403 to Y.Y.).

Authorship

Contribution: K.U., K.N., M.W., and B.C.T. designed research; K.U., T.S., D.E.K., and D.C.B. performed research; M.L. provided vital reagents; C.A.S. served as research coordinator and obtained all the clinical samples from normal volunteers; J.P.K., K.U., and B.C.T. analyzed the data; and K.U., K.N., B.C.C., L.A.D., N.K., Y.Y., and B.C.T. wrote the manuscript.

Conflict-of-interest disclosure: The authors declare no competing financial interests.

Correspondence: Bruce C. Trapnell, MD, Division of Pulmonary Biology, Cincinnati Children's Hospital Medical Center, 3333 Burnet Avenue, Cincinnati, OH 45229-3039; e-mail: bruce.trapnell@cchmc.org

References

1. Shibata Y, Berclaz PY, Chroneos ZC, Yoshida M, Whitsett JA, Trapnell BC. GM-CSF regulates alveolar macrophage differentiation and innate immunity in the lung through PU. 1. Immunity. 2001; 15:557-567.
2. Hamilton JA, Anderson GP. GM-CSF Biology. Growth Factors. 2004;22:225-231.
3. Trapnell BC, Whitsett JA. GM-CSF regulates pulmonary surfactant homeostasis and alveolar macrophage-mediated innate host defense. Annu Rev Physiol. 2002;64:775-802.
4. Trapnell BC, Whitsett JA, Nakata K. Pulmonary Alveolar Proteinosis. N Engl J Med. 2003;349: 2527-2539.
5. Uchida K, Beck DC, Yamamoto T, et al. GM-CSF autoantibodies and neutrophil dysfunction in pulmonary alveolar proteinosis. N Engl J Med. 2007; 356:567-579.
6. Ruef C, Coleman DL. Granulocyte-macrophage colony-stimulating factor: pleiotropic cytokine with potential clinical usefulness. Rev Infect Dis. 1990; 12:41-62.
7. Huffman Reed JA, Rice WR, Zsengeller ZK, Wert SE, Dranoff G, Whitsett JA. GM-CSF enhances lung growth and causes alveolar type II epithelial cell hyperplasia in transgenic mice. Am J Physiol. 1997;273:L715-725.
8. Freedman MH, Grunberger T, Correa P, Axelrad AA, Dube ID, Cohen A. Autocrine and paracrine growth control by granulocyte-monocyte colony-stimulating factor of acute lymphoblastic leukemia cells. Blood. 1993;81:3068-3075.
9. Yamaoka K, Otsuka T, Niiro H, et al. Activation of STAT5 by lipopolysaccharide through granulocyte-macrophage colony-stimulating factor production in human monocytes. J Immunol. 1998; 160:838-845.
10. Graves V, Gabig T, McCarthy L, Strour EF, Leemhuis T, English D. Simultaneous mobilization of Mac-1 (CD11b/CD18) and formyl peptide chemoattractant receptors in human neutrophils. Blood. 1992;80:776-787.
11. Hansen G, Hercus TR, McClure BJ, et al. The structure of the GM-CSF receptor complex reveals a distinct mode of cytokine receptor activation. Cell. 2008;134:496-507.
12. Guthridge MA, Powell JA, Barry EF, et al. Growth factor pleiotropy is controlled by a receptor Tyr/Ser motif that acts as a binary switch. EMBO J. 2006;25:479-489.
13. Carraway MS, Ghio AJ, Carter JD, Piantadosi CA. Detection of granulocyte-macrophage colony-stimulating factor in patients with pulmonary alveolar proteinosis. Am J Respir Crit Care Med. 2000;161:1294-1299.
14. Dranoff G, Crawford AD, Sadelain M, et al. Involvement of granulocyte-macrophage colony-stimulating factor in pulmonary homeostasis. Science. 1994;264:713-716.
15. Stanley E, Lieschke GJ, Grail D, et al. Granulocyte/macrophage colony-stimulating factor-deficient mice show no major perturbation of hematopoiesis but develop a characteristic pulmonary pathology. Proc Natl Acad Sci U S A. 1994;91: 5592-5596.

16. Ikegami M, Ueda T, Hull W, et al. Surfactant metabolism in transgenic mice after granulocyte macrophage-colony stimulating factor ablation. Am J Physiol. 1996;270:L650-658.
17. Seymour JF, Lieschke GJ, Grail D, Quilici C, Hodgson G, Dunn AR. Mice lacking both granulocyte colony-stimulating factor (CSF) and granulocyte-macrophage CSF have impaired reproductive capacity, perturbed neonatal granulopoiesis, lung disease, amyloidosis, and reduced long-term survival. Blood. 1997;90:3037-3049.
18. Seymour JF, Presneill JJ. Pulmonary alveolar proteinosis: progress in the first 44 years. Am J Respir Crit Care Med. 2002;166:215-235.
19. Kitamura T, Tanaka N, Watanabe J, et al. Idiopathic pulmonary alveolar proteinosis as an autoimmune disease with neutralizing antibody against granulocyte/macrophage colony-stimulating factor. J Exp Med. 1999;190:875-880.
20. Uchida K, Nakata K, Trapnell BC, et al. High-affinity autoantibodies specifically eliminate granulocyte-macrophage colony-stimulating factor activity in the lungs of patients with idiopathic pulmonary alveolar proteinosis. Blood. 2004;103: 1089-1098.
21. Lang RA, Metcalf D, Cuthbertson RA, et al. Transgenic mice expressing a hemopoietic growth factor gene (GM-CSF) develop accumulations of macrophages, blindness, and a fatal syndrome of tissue damage. Cell. 1987;51:675-686.
22. Jang J, Lim DS, Choi YE, et al. MLN51 and GM-CSF involvement in the proliferation of fibroblast-like synoviocytes in the pathogenesis of rheumatoid arthritis. Arthritis Res Ther. 2006;8:R170.
23. McQualter JL, Darwiche R, Ewing C, et al. Granulocyte macrophage colony-stimulating factor: a new putative therapeutic target in multiple sclerosis. J Exp Med. 2001;194:873-882.
24. Hamilton JA. GM-CSF in inflammation and autoimmunity. Trends Immunol. 2002;23:403-408.
25. Svenson M, Hansen MB, Ross C, et al. Antibody to granulocyte-macrophage colony-stimulating factor is a dominant anti-cytokine activity in human IgG preparations. Blood. 1998;91:2054-2061.
26. Bendtzen K, Svenson M, Hansen MB, et al. GM-CSF autoantibodies in pulmonary alveolar proteinosis. N Engl J Med. 2007;356:2001-2002.
27. Inoue Y, Trapnell BC, Tazawa R, et al. Characteristics of a large cohort of autoimmune pulmonary alveolar proteinosis patients in Japan. Am J Respir Crit Care Med. 2008.
28. Kurdowska A, Miller EJ, Noble JM, et al. Anti-IL-8 autoantibodies in alveolar fluid from patients with the adult respiratory distress syndrome. J Immunol. 1996;157:2699-2706.
29. Watanabe M, Uchida K, Nakagaki K, et al. Anti-cytokine autoantibodies are ubiquitous in healthy individuals. FEBS Lett. 2007;581:2017-2021.
30. Kitamura T, Uchida K, Tanaka N, et al. Serological diagnosis of idiopathic pulmonary alveolar proteinosis. Am J Respir Crit Care Med. 2000;162: 658-662.
31. Seymour JF, Doyle IR, Nakata K, et al. Relationship of anti-GM-CSF antibody concentration, surfactant protein A and B levels, and serum LDH to pulmonary parameters and response to GM-CSF therapy in patients with idiopathic alveolar proteinosis. Thorax. 2003;58:252-257.
32. Berclaz PY, Shibata Y, Whitsett JA, Trapnell BC. GM-CSF, via PU. 1, regulates alveolar macrophage Fcgamma R-mediated phagocytosis and the IL-18/IFN-gamma -mediated molecular connection between innate and adaptive immunity in the lung. Blood. 2002;100:4193-4200.
33. Perkins DN, Pappin DJ, Creasy DM, Cottrell JS. Probability-based protein identification by searching sequence databases using mass spectrometry data. Electrophoresis. 1999;20:3551-3567.
34. Mascot Search: Matrix Science Ltd.; 1997.
35. Steindl F, Armbruster C, Pierer K, Purtscher M, Katinger HW. A simple and robust method for the complete dissociation of HIV-1 p24 and other antigens from immune complexes in serum and plasma samples. J Immunol Methods. 1998;217: 143-151.
36. Zsengeller Z, Otake K, Hossain SA, Berclaz PY, Trapnell BC. Internalization of adenovirus by alveolar macrophages initiates early proinflammatory signaling during acute respiratory tract infection. J Virol. 2000;74:9655-9667.
37. Berclaz PY, Zsengeller Z, Shibata Y, et al. Endocytic internalization of adenovirus, nonspecific phagocytosis, and cytoskeletal organization are coordinately regulated in alveolar macrophages by GM-CSF and PU. 1. J Immunol. 2002;169: 6332-6342.
38. Gonzalez-Juarrero M, Hattle JM, Izzo A, et al. Disruption of granulocyte macrophage-colony stimulating factor production in the lungs severely affects the ability of mice to control Mycobacterium tuberculosis infection. J Leukoc Biol. 2005; 77:914-922.
39. Presneill JJ, Nakata K, Inoue Y, Seymour JF. Pulmonary alveolar proteinosis. Clin Chest Med. 2004;25:593-613, viii.
40. Meager A, Wadhwa M, Bird C, et al. Spontaneously occurring neutralizing antibodies against granulocyte-macrophage colony-stimulating factor in patients with autoimmune disease. Immunology. 1999;97:526-532.
41. Sayani F, Montero-Julian FA, Ranchin V, et al. Identification of the soluble granulocyte-macrophage colony stimulating factor receptor protein in vivo. Blood. 2000;95:461-469.
42. Bozinovski S, Jones J, Beavitt SJ, Cook AD, Hamilton JA, Anderson GP. Innate immune responses to LPS in mouse lung are suppressed and reversed by neutralization of GM-CSF via repression of TLR-4. Am J Physiol Lung Cell Mol Physiol. 2004;286:L877-885.
43. Ross C, Svenson M, Hansen MB, Vejlsgaard GL, Bendtzen K. High avidity IFN-neutralizing antibodies in pharmaceutically prepared human IgG. J Clin Invest. 1995;95:1974-1978.
44. Bendtzen K, Hansen MB, Ross C, Svenson M. High-avidity autoantibodies to cytokines. Immunol Today. 1998;19:209-211.
45. Metcalf D, Nicola NA, Mifsud S, Di Rago L. Receptor clearance obscures the magnitude of granulocyte-macrophage colony-stimulating factor responses in mice to endotoxin or local infections. Blood. 1999;93:1579-1585.
46. Finkelman FD, Madden KB, Morris SC, et al. Anti-cytokine antibodies as carrier proteins. Prolongation of in vivo effects of exogenous cytokines by injection of cytokine-anti-cytokine antibody complexes. J Immunol. 1993;151:1235-1244.
47. Zaheer A, Zaheer S, Sahu SK, Yang B, Lim R. Reduced severity of experimental autoimmune encephalomyelitis in GMF-deficient mice. Neurochem Res. 2007;32:39-47.
48. Ponomarev ED, Shriver LP, Maresz K, Pedras-Vasconcelos J, Verthelyi D, Dittel BN. GM-CSF production by autoreactive T cells is required for the activation of microglial cells and the onset of experimental autoimmune encephalomyelitis. J Immunol. 2007;178:39-48.
49. Krinner EM, Raum T, Petsch S, et al. A human monoclonal IgG1 potently neutralizing the pro-inflammatory cytokine GM-CSF. Mol Immunol. 2007;44:916-925.

Tuberculosis 89 (2009) 71–76

Contents lists available at ScienceDirect

Tuberculosis

journal homepage: http://intl.elsevierhealth.com/journals/tube

No evidence for association between the interferon regulatory factor 1 (*IRF1*) gene and clinical tuberculosis

Sabine Vollstedt [a,b,g], Rika Yuliwulandari [b,c,g], Koji Okamoto [d], Luu Thi Lien [e], Naoto Keicho [f], Jecti Teguh Rochani [c], Riyani Wikaningrum [c], Katsushi Tokunaga [b,*]

[a] Department of Immunology, Graduate School of Medicine and Faculty of Medicine, University of Tokyo, Japan
[b] Department of Human Genetics, Graduate School of Medicine, University of Tokyo, Japan
[c] Faculty of Medicine, Yarsi University, Jakarta, Indonesia
[d] Department of Nephrology and Endocrinology, Graduate School of Medicine, University of Tokyo, Japan
[e] Hanoi Tuberculosis and Lung Disease Hospital, Hanoi, Viet Nam
[f] Department of Respiratory Diseases, Research Institute, International Medical Centre of Japan, Tokyo, Japan

ARTICLE INFO

Article history:
Received 7 March 2008
Received in revised form 21 August 2008
Accepted 24 September 2008

Keywords:
Tuberculosis
Interferon regulatory factor 1 (IRF1)

SUMMARY

Interferon regulatory factor 1 is a transcription factor involved in initiating a vigorous Th1 response during *Mycobacterium tuberculosis* infection. Therefore, we considered it as a possible candidate gene for certain polymorphisms to confer susceptibility to develop clinical tuberculosis. However, all polymorphisms with minor allele frequencies higher than 5% and haplotype frequencies in two Southeast Asian populations (Indonesian and Vietnamese) turned out not to be associated with pulmonary tuberculosis.

1. Introduction

Tuberculosis (TB) is still a major health problem worldwide. Although, it is mainly active in developing countries, it obtained a new impact in developed countries when linked to immune suppressions as for example after HIV infections.[48,7] About one third of the world's population is predicted to be infected by *Mycobacterium tuberculosis (M. tuberculosis)*[11] and it causes nearly 2 million deaths per year. However, of all infected subjects, only 5–10% develop clinical disease.[49]

The immune mechanisms in TB are well studied and it is known that the IL-12/IFN-γ axis plays a major role for the control and elimination of *M. tuberculosis*.[45,46] Although T cells, especially γδ T cells, are involved during the immune response,[16] macrophages play one of the most important roles and their activation status is crucial for controlling the infection.

During the last few years, resistance to tuberculosis was found to be connected to specific polymorphisms of genes of some of the major immune components. Specific single nucleotide polymorphisms (SNPs) in the *IL-12* or IL-12 receptor (*IL-12R*) gene, for instance, were related to higher susceptibility of tuberculosis.[3] Specific alleles of the *IFNG* gene led to higher amounts of IFN-γ,[30] and the presence of a low IFN-g producing genotype was overpresented in tuberculosis-infected patients.[44] Defects of the IFN-γ receptor led to higher susceptibility of mycobacterial infections,[17] and some alleles of the *IFNG* gene were associated to disease.[10,25,34] SNPs directly affecting the genes of macrophage activation, such as *SP110* in human[42] homologue to *Ipr1* in mice[29] and *MIF* (macrophage inhibitory factor)[13] first discovered as a proinflammatory T-cell cytokine[26] were also shown to have an impact in the control and elimination of mycobacterial infection.

Although some important factors for mycobacterial resistance are already known, it is essential to learn more about the fine tuning of the immune response in order to have better tools for manipulating the immune system in areas with a high incidence of mycobacterial infections such as Indonesia that ranks 3rd among 22-high burden TB countries in the world. In this regard, transcription factors play a very important role. Interferon regulatory factors (IRFs) are known to be important for the initiation and fine tuning of immune responses.[36,47] IRFs are a tightly regulatory network of gene regulation for genes that are important for antibacterial immunity.[14,40,41] Among those, IRF1 is known to play an important role in promoting an anti-bacterial immune response by

* Corresponding author. Department of Human Genetics, Graduate School of Medicine, University of Tokyo, 7-3-1, Hongo, Bunkyo-ku, Tokyo 113-0033, Japan. Tel.: +81 3 58413692; fax: +81 3 5802 2907.
E-mail address: tokunaga@m.u-tokyo.ac.jp (K. Tokunaga).
[g] Both the authors contributed equally.

1472-9792/$ – see front matter © 2008 Elsevier Ltd. All rights reserved.
doi:10.1016/j.tube.2008.09.006

targeting *NOS2*, *GBP1* and *gp91PHOX* genes,[18,21] promoting a vigorous cellular response by targeting IL-12[39] and IL-18,[9] influencing the hematopoietic cell development by targeting IL-15.[27] MyD88 associated IRF1 is a potent activator for IFN-β, NOS and IL-12p35.[24] IRF1 is essential to develop a T helper type 1 (Th1) response[22] and, thus, is important during *M. tuberculosis* infection.[31,33] It was also up-regulated upon infection with *M. tuberculosis* in the mice.[20] Therefore, we chose this transcription factor as our target gene to examine their possible association to the susceptibility to TB.

Human *IRF1* gene is a minus strand spanning 7.72 kb with a 495 bp promoter region and it has been assigned to 5q31.1,[14] a region contains the cytokine gene cluster and is frequently deleted in the malignant cells of patients with myelodysplasia and myeloid leukemia.[4] It encodes a 36.5 kDa protein. *IRF1* genomic sequence consists of 10 exons and there are 94 SNPs reported in publicly accessible genome database/GenBank.

2. Material and methods

2.1. Patients and control subjects

A case-control study was designed in 2006 by using diagnosed pulmonary TB patients ($n = 192$) from the West Java province of Indonesia. The patients were between the ages of 15 and 68 years old and their ethnic background was Javanese and Sundanese–Javanese, West Java with comparable sex ratio. Diagnosis of TB was based upon the presence of clinical symptoms, chest X-rays and microscopic detection of acid-fast bacilli in Ziehl–Nehlsen stained sputum smear.

In the same period, community healthy controls were collected from people of the same age, gender and area ($n = 192$). Controls had the same interview with standard questions and underwent the same physical examinations. Investigations were approved by the Ethical Committees of Yarsi University, Jakarta, Indonesia and Graduate School of Medicine, University of Tokyo, Tokyo, Japan.

In the study of the Vietnamese population, 162 pulmonary TB patients underwent similar physical and laboratory examinations for TB as Indonesian were recruited to participate. As control, 132 healthy unrelated subjects were randomly selected from 20 communes of Hanoi, Vietnam, and blood samples were taken after obtaining the informed consent from each subject. Ethical approval for this research was obtained from the ethical committees of both the Ministry of Health of Vietnam and the International Medical Center of Japan.

2.2. Variation screening and Genotyping of SNPs on IRF1

Genomic DNA was extracted from peripheral blood using a commercial kit (QiaAmp Blood Mini Kit, Qiagen). Polymerase chain reactions were performed in a final volume of 15 μl, containing 10 ng genomic DNA, 1.5 pmol of each primer, 2 mM of dNTP, 10× PCR buffer, 5× GC-rich solution and 0.6 U FastStart Taq Polymerase (Roche Applied Science, Mannheim, Germany). Each PCR was performed with a hot-start procedure at 95 °C for 10 min. The amplification process was carried out using 40 cycles of denaturation at 94 °C for 1 min, with annealing temperature between 59.2 °C and 62.9 °C for 30 s, and elongation at 72 °C for 1 min followed by a final elongation at the last cycle at 72 °C for 10 min.

Table 1
Genome-specific primer pairs with the location on the gene and the direction.

Gene Region	Abbr.	Sense (5′ → 3′)	Antisense (5′ → 3′)
Promoter region	P	ccccttctcctcctctgttc	ttgcctcgactaaggagtgg
Exon1/intron1	E1I1	ctcgccactcctagtcgag	aaaggcgtactcacctctgc
Intron1/exon2/intron2	I1I2	gtcaggaaggcgtagaatgg	ccagagtgactggtgcaaga
Intron2	I2	ggcttagcagaggacaaacg	cacagactttggggctgagt
Exon3/intron3	E3I3	gtctcagactcagccccaaa	cagagagccacagtggtcaa
Intron4	I4	ctggcaaaagcatctgtgaa	cagagagccacagtggtcaa
Exon4/exon5/exon6/intron6	E4I6	agtgtcaccgggagtacctg	ccacaggtcaaggttgtgtg
Exon7/exon8/intron7	E7I7	gctgtcagcagcactctcc	ctgtactgcagcccactctg
Intron8	I8	tgggtagctgctgttgtcac	tggccattttcacaatctca
Intron8/exon9/exon10	I9E10	aaatggccaagggtgtgata	gctcagaggaaaaagc
Intron9	I9	gaaccacgtagggatggaga	aggtggcatccatgttcttc

Part of the PCR products was subjected to electrophoresis in a 2% agarose gel to verify specific amplification. After purification of the PCR product using 10 U Exo1 and 1 U Sap, direct sequencing was performed using a commercial kit (BigDye Terminator ver. 3.1, Applied Biosystems) with an automated sequencer (ABI 3730, Applied Biosystems).

Variation screening was done using 192 Indonesian controls. All exons and introns of *IRF1* as well as the promoter region (−500 bp to 0 bp) were read by direct sequencing. Then, only SNPs that had minor allele frequencies over 5% were genotyped in all case and control subjects. The specific primers used for variation screening and genotyping were listed in Table 1. Primers I4 and I9 were used only for re-genotyping of low called SNPs.

The promoter region of *IRF1* seemed to be one of the most promising sites for TB associated SNPs,[38] because it potentially influenced the outcome of a Th1 response during viral infection.[35] There were numeral GC-rich boxes with SP1 and NF-κB binding.[38] Therefore, we used samples of the Vietnamese population to double-check the five polymorphisms in the promoter, which had a minor allele frequency higher than 5%.

2.3. Statistical analysis

Allele and genotype frequencies were checked for deviation from the Hardy–Weinberg equilibrium and the differences of allele and genotype frequencies between cases and controls were analyzed. Haplotype frequencies were estimated by the maximum-likelihood method using the Haploview ver. 4.1 software. The haplotype structure with linkage disequilibrium (LD) values was also constructed using the same software. The permutation p value was calculated with 5000× permutation test.

Association analysis was done using the chi-square test. Meta-analysis on the promoter alleles in Indonesian and Vietnamese was also done using a previously described method.[23] The statistical power was assessed according to disease prevalence, minor allele frequency, significant level and odds ratio according to our previous study.[28]

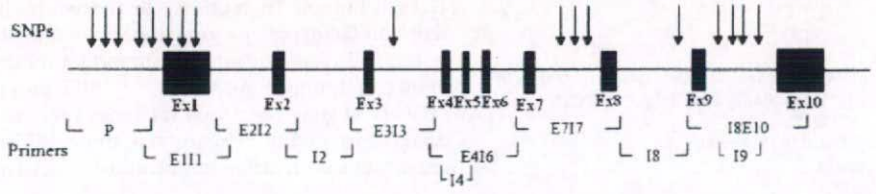

Figure 1. Structure of the *IRF1* gene. Gene structure including exons and introns with the sites of the 17 SNPs and the annealing position of the primers.

Table 2
Location and frequency of *IRF1* SNP alleles and genotypes in Indonesian case and control samples.

Name	Location	Allele or genotype	Frequency in cases (%)	Frequency in controls (%)	p-Value
rs2549005	Promoter	G	243 (63.9)	244 (67)	0.376
		A	137 (36)	120 (32.9)	
		GG	75 (39.4)	77 (40.1)	0.626
		GA	93 (48.9)	87 (45.3)	
		AA	22 (11.5)	28 (14.6)	
rs2549006	Promoter	C	243 (63.9)	244 (67)	0.376
		T	137 (36)	120 (32.9)	
		CC	75 (39.4)	76 (39.5)	0.652
		CT	93 (48.9)	88 (45.8)	
		TT	22 (11.5)	28 (14.6)	
rs2706384	Promoter	A	241 (63.7)	240 (62.5)	0.719
		C	137 (36.2)	144 (37.5)	
		AA	74 (39.1)	76 (39.5)	0.649
		AC	93 (49.2)	88 (45.8)	
		CC	22 (11.6)	28 (14.5)	
rs2549007	Promote	G	241 (63.7)	241 (62.7)	0.775
		A	137 (36.2)	143 (37.2)	
		GG	74 (39.1)	77 (40.1)	0.618
		GA	93 (49.2)	87 (45.3)	
		AA	22 (11.6)	28 (14.5)	
rs2549008	Promoter	C	324 (90.5)	327 (90.8)	0.879
		T	34 (9.4)	33 (9.1)	
		CC	145 (81)	147 (81.6)	0.872
		CT	34 (18.9)	33 (18.3)	
		TT	0 (0)	0 (0)	
rs1124211	Exon 1	C	357 (93.0)	360 (93.8)	0.055
		G	25 (6.5)	18 (4.7)	
		CC	167 (87.0)	174 (90.6)	0.137
		CG	23 (12.0)	12 (6.3)	
		GG	1 (0.5)	3 (1.6)	
rs10900809	Exon 1	C	253 (65.9)	238 (62.0)	0.400
		T	131 (34.1)	140 (36.5)	
		CC	82 (42.7)	77 (40.1)	0.258
		CT	89 (46.4)	84 (43.8)	
		TT	21 (10.9)	28 (14.6)	
rs960757	Exon 1	C	357 (93.0)	360 (93.8)	0.288
		T	25 (6.5)	18 (4.7)	
		CC	167 (87.0)	174 (90.6)	0.137
		CT	23 (12.0)	12 (6.3)	
		TT	1 (0.5)	3 (1.6)	
rs2070723	Intron 3	T	244 (63.5)	231 (60.1)	0.211
		C	134 (34.9)	153 (39.8)	
		TT	78 (40.6)	74 (38.5)	0.100
		TC	88 (45.8)	83 (43.2)	
		CC	23 (12.0)	35 (18.2)	
rs10214312	Intron 7	A	251 (65.4)	238 (62.0)	0.378
		C	133 (34.6)	144 (37.5)	
		AA	82 (42.7)	78 (40.6)	0.232
		AC	87 (45.3)	82 (42.7)	
		CC	23 (12.0)	31 (16.1)	
rs2070725	Intron 7	G	249 (64.8)	236 (61.5)	0.379
		A	135 (35.2)	146 (38.0)	
		GG	82 (42.7)	71 (37.0)	0.269
		GA	85 (44.3)	94 (49.0)	
		AA	25 (13.0)	26 (13.5)	
rs17848415	Intron 7	A	241 (64.4)	236 (62.4)	0.568
		C	133 (35.5)	142 (37.5)	
		AA	76 (40.6)	74 (39.1)	0.468
		AC	89 (47.5)	88 (46.5)	
		CC	22 (11.7)	27 (14.2)	
rs2070727	Intron 8	G	241 (64.4)	233 (61.6)	0.427
		T	133 (35.5)	145 (38.3)	
		GG	76 (40.6)	72 (38)	0.384
		GT	89 (47.5)	89 (47)	
		TT	22 (11.7)	28 (14.8)	
rs2070728	Intron 9	G	239 (64.2)	235 (62.1)	0.555
		A	133 (35.7)	143 (37.8)	
		GG	75 (40.3)	73 (38.6)	0.480
		GA	89 (47.8)	89 (47)	
		AA	22 (11.8)	27 (14.2)	
rs7701588	Intron 9	T	235 (61.2)	245 (63.8)	0.301
		C	149 (38.8)	133 (34.6)	
		TT	72 (37.5)	77 (40.1)	0.248
		TC	91 (47.4)	91 (47.4)	
		CC	29 (15.1)	21 (10.9)	
rs2070729	Intron 9	T	247 (64.3)	233 (60.7)	0.443
		G	137 (35.7)	145 (37.8)	
		TT	78 (40.6)	74 (38.5)	0.272
		TG	91 (47.4)	85 (44.3)	
		GG	23 (12.0)	30 (15.6)	
rs2070730	Intron 9	C	247 (64.3)	233 (60.7)	0.443
		T	137 (35.7)	145(37.8)	
		CC	78 (40.6)	74 (38.5)	0.272
		CT	91 (47.4)	85 (44.3)	
		TT	23 (12.0)	30 (15.6)	

3. Results

3.1. Variation screening and association analyses in the Indonesian population

Of the 94 SNPs registered in the *IRF* gene in GenBank database, only 17 of those SNPs had a minor allele frequency over 5% and these SNPs were subjected to analysis for a possible association with clinical TB. No polymorphisms were newly discovered. Of these 17 SNPs, five were found in the promoter region, three were in exon 1, one was in intron 3, three was in intron 7, one was in intron 8 and the last four were situated in intron 9 (Figure 1). All polymorphisms were in accordance with the Hardy–Weinberg equilibrium (data not shown). Their description, location and allele frequency were shown in Table 2. Any single SNP did not show significant association with the disease.

3.2. Haplotype analyses in the Indonesian population

Haploblocks were constructed according to solid spine method (Figure 2). The first block consisted of the six SNPs composed of three SNPs of intron 10, one of intron 9 and two of intron 8. The second block was constructed from the remaining SNPs. The haplotype blocks were mapped in Table 3. Of the haplotype blocks, 6 tag SNPs (rs2070730, rs7701588, rs2070727 in the block 1 and rs2070725, rs960757, rs2549005 in the block 2) were selected for further association analyses (Figure 2).

Strong LD was observed in most region of the gene involving all the 17 SNPs. Four pairs of SNPs (rs2070730 and rs2070729, rs960757 and rs11242115, rs2549008 and rs2549005 and rs2706384 and rs2549006) showed complete LD with $r^2 = 1$. In the promoter region, all 5 SNPs showed maximal LD with $D' = 1$ (Figure 2). LD and haplotype analyses were carried out based on the genotypes of 17 SNPs in control and case samples. There was no significant association between any haplotype and TB (Table 3).

3.3. Association analyses in the Vietnamese population

Five polymorphisms in the promoter region were analyzed also in Vietnamese samples. Similar as in the Indonesian samples, there was no association between the polymorphisms and the disease (Table 4). LD structure and haplotype structure were well preserved

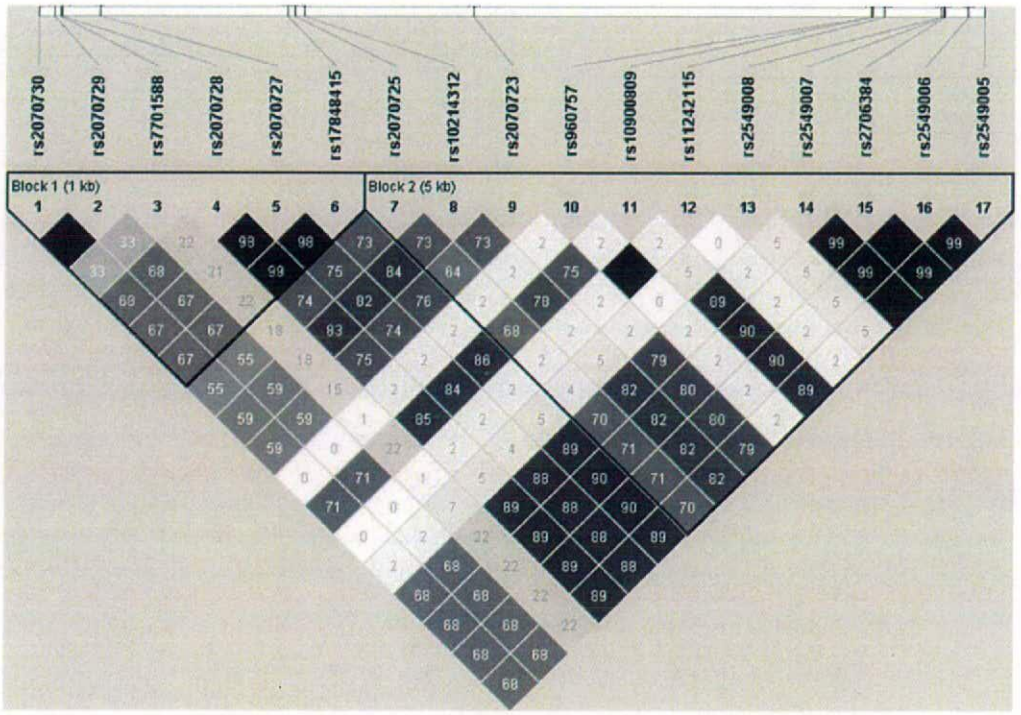

Figure 2. Haplotype block structure in the *IRF1* gene in Indonesian. The extent of the LD (r^2) between SNPs is shown by the color of the box, where black boxes indicate a high r^2 (with the percentage written inside) and white boxes showing a lower r^2. SNPs number 1, 3, 5, 7, 10 and 13 were selected as tag SNPs.

as Indonesian samples (Figure 3), and no haplotype was found to be associated with TB (Table 4).

3.4. Meta-analysis of promoter polymorphisms

Using 5 SNPs found in the promoter region, we also performed meta-analysis on both data of Indonesian and Vietnamese (Table 5). All promoter SNPs showed no significant association with tuberculosis as well.

4. Discussion

Pathogenesis of TB has been extensively studied, however, lack of understanding of the details of how the immune response mechanisms control and eliminate the pathogen is still remained,[45,46] resulting the disease as a major cause of death worldwide and as a single agent surpassed only by malaria in the number of deaths per year.[49]

During an immune response there are numeral cells involved during the recognition and activation phase, as well as in the

Table 3
Haplotype frequency in Indonesian case and control samples.

Haplotype	Frequency in cases (%)	Frequency in controls (%)	Permutation *p*-value
Block 1 (rs2070730–rs7701588–rs2070727)			
C–C–G	38.3	30.0	0.1782
T–T–T	34.0	31.3	0.9980
C–T–G	24.5	24.8	1.0000
T–T–G	1.6	7.0	0.0036
Block 2 (rs2070725–rs960757–rs2549008)			
G–C–T	45.7	41.4	1.0000
A–C–C	31.7	28.3	0.9914
G–C–C	8.3	7.0	0.9740
G–T–C	6.5	3.8	0.6368

Table 4
Location and frequency of *IRF1* promoter SNP alleles, genotypes and haplotypes in Vietnamese case and control samples.

Name	Location	Allele or genotype	Frequency in cases (%)	Frequency in control (%)	*p*-Value
rs2549005	Promoter	G	182 (56.2)	160 (60.6)	0.278
		A	142 (43.8)	104 (39.4)	
		GG	57 (35.2)	50 (37.9)	0.421
		GA	68 (42.0)	60 (45.5)	
		AA	37 (22.8)	22 (16.7)	
rs2549006	Promoter	C	182 (56.2)	158 (59.8)	0.369
		T	142 (43.8)	106 (40.2)	
		CC	57 (35.2)	49 (37.1)	0.516
		CT	68 (42.0)	60 (45.5)	
		TT	37 (22.8)	23 (17.4)	
rs2706384	Promoter	A	182 (56.2)	160 (60.6)	0.278
		C	142 (43.8)	104 (39.4)	
		AA	57 (35.2)	50 (37.9)	0.421
		AC	68 (42.0)	60 (45.5)	
		CC	37 (22.8)	22 (16.7)	
rs2549007	Promoter	G	181 (55.9)	160 (60.6)	0.247
		A	143 (44.1)	104 (39.4)	
		GG	56 (34.6)	50 (37.9)	0.419
		GA	69 (42.6)	60 (45.5)	
		AA	37 (22.8)	22 (16.7)	
rs2549008	Promoter	C	295 (91.0)	239 (90.5)	0.942
		T	29 (9.0)	23 (8.7)	
		CC	135 (83.3)	109 (82.6)	0.917
		CT	25 (15.4)	21 (15.9)	
		TT	2 (1.2)	1 (0.8)	

rs2549008-rs2549007	Frequency in cases (%)	Frequency in controls (%)	Permutation *p*-value
C–G	89.8	96.4	0.7990
C–A	76.7	64.5	0.7824
T–G	9.2	9.8	1.0000

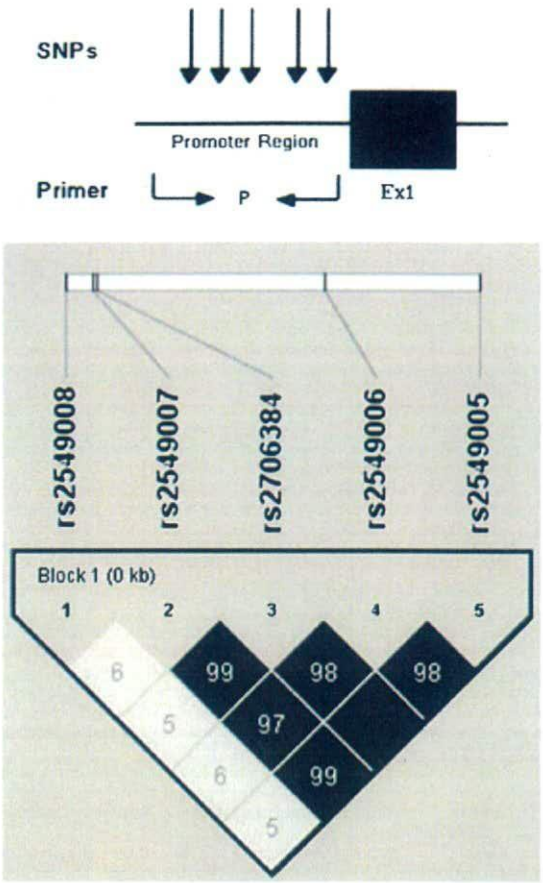

Figure 3. Haplotype structure of polymorphisms found in the promoter of the *IRF1* gene in Vietnamese. The extent of the LD (r^2) between SNPs is shown by the color of the box, where black boxes indicate a high r^2 (with the percentage written inside) and white boxes showing a lower r^2. SNPs number 1 and 2 were selected as tag SNPs.

Table 5
Meta-analysis of *IRF1* promoter polymorphisms in Indonesian and Vietnamese.

Name	Location	Allele or genotype	Frequency in cases (%)	Frequency in control (%)	*p*-Value
rs2549005	Promoter	G	425 (60.4)	404 (64.3)	0.137
		A	279 (39.6)	224 (35.7)	
		GG	132 (37.5)	127 (39.2)	0.854
		GA	161 (45.7)	147 (45.4)	
		AA	59 (16.8)	50 (15.4)	
rs2549006	Promoter	C	425 (60.4)	402 (64.0)	0.171
		T	279 (39.6)	226 (36.0)	
		CC	132 (37.5)	125 (38.6)	0.923
		CT	161 (45.7)	148 (45.7)	
		TT	59 (16.8)	51 (15.7)	
rs2706384	Promoter	A	423 (60.3)	400 (61.7)	0.580
		C	279 (839.7)	248 (38.3)	
		AA	131 (37.3)	126 (38.9)	0.857
		AC	161 (45.9)	148 (45.7)	
		CC	59 (16.8)	50 (15.4)	
rs2549007	Promoter	G	422 (60.1)	401 (61.9)	0,506
		A	280 (39.9)	247 (38.1)	
		GG	130 (37.0)	127 (39.2)	0.808
		GA	162 (46.2)	147 (45.4)	
		AA	59 (16.8)	50 (15.4)	
rs2549008	Promoter	C	619 (90.8)	566 (91.0)	0.883
		T	63 (9.2)	56 (9.0)	
		CC	280 (82.1)	256 (82.3)	0.883
		CT	59 (17.3)	54 (17.4)	
		TT	2 (0.6)	1 (0.3)	

effector phase. Dendritic cells (DC) and macrophages recognize the pathogen by their innate pattern recognition receptors, especially toll-like receptor (TLR) 2 and 4.[32,1,8,6] This leads to an early production of IL-12 and TNF-α, which in turn activates natural killer (NK) cells to produce IFN-γ.[15,43,2] Antigen-presenting cells also migrate to the lymph nodes to activate naïve T cells. This, together with high production of IL-12, leads to a Th1 immune response. These T cells are responsible for high amounts of IFN-γ production during the adaptive phase.[15] IFN-γ together with TNF-α is very important in the activation of macrophages, especially when they are infected by *M. tuberculosis*.[46]

This knowledge helped to investigate specific components of the immune system for polymorphisms. Indeed, polymorphisms in *IL-12*,[34] *IL-12R*,[3] *IFNG*,[30,44] *IFNGR*[17,10,25,34] and in effector functions of macrophages[29,42] led to an increased susceptibility to TB.

Although knowledge has expanded considerably, it is still not enough to control infection and disease. For this goal we need more insights into how these components and cytokines are regulated and how to use this knowledge as tools to manipulate the immune systems for vaccinations and treatments. In this study we approached this question by analyzing *IRF1* gene. This transcription factor does not only play an important role in the induction of IL-12,[39] an early component for a vigorous Th1 response, it is also essential for NK cell development[27] and during T cell differentiation itself.[22] However, our study showed that polymorphisms in this gene did not play a role in the outcome of clinical TB. Using 192 samples each for case and control of Western Javanese Indonesia with the incidence of TB 100/100,000 population per year, we found that 90% of statistical power with a significance level of 0.05 will be obtained if the susceptible allele showing OR > 1.63 with average MAF of 31%.[28] Or in other words, at least 143 samples each are needed for case and control to get statistical power >80% in the studied population. In this study, both populations showed neither single polymorphisms nor specific haplotypes led to an increased susceptibility to TB. Since the control samples in Vietnamese were only 132, this insignificant result could be due to low statistical power resulted from the small sample size. Then we also did meta-analysis of SNPs in promoter region in both Indonesian and Vietnamese population. Again no significant results were shown. Therefore, it is likely that the result of this study could produce conclusive result.[5] This is not surprising because transcription factors such as IRFs are redundant to some extent. IRF5 for example is another factor, which plays an important role in developing a Th1 response. Polymorphisms in *IRF5* gene have been reported to be associated with susceptibility to systemic lupus erythematosus.[12,19,37] However, thus far no reports have been published on its possible association with TB.

Although there was no association between polymorphisms in *IRF1* gene and TB, this transcription factor plays an important role in the transcription of *IL-12* which leads to the activation of Th1 cells essential for host defense mechanisms against TB. Investigations on the other transcription factors related to the immune pathway would be worthy to further elucidate the pathogenesis of TB. In addition, it is very important that research in this field should be continued in order to learn more about the subtle regulations of the immune response and, to gain knowledge for efficiently prohibiting the fatal outcome of this pathogen's activity.

Acknowledgement

This work was supported by Grant-in-Aid for Scientific Research on Priority Areas "Comprehensive Genomics" from the Ministry of Education, Culture, Sports, Science and Technology of Japan and by Japanese Society for the Promotion of Science (JSPS).

Funding: Grant-in-Aid for Scientific Research on Priority Areas "Comprehensive Genomics" from the Ministry of Education, Culture, Sports, Science and Technology of Japan and Japanese Society for the Promotion of Science (JSPS).

Competing interests: None declared.

Ethical approval: Ethical committees of Faculty of Medicine, Yarsi University, Jakarta, Indonesia and Graduate School of Medicine, The University of Tokyo, Tokyo, Japan.

References

1. Abel B, Thieblemont N, Quesniaux VJ, Brown N, Mpagi J, Miyake K, et al. Toll-like receptor 4 expression is required to control chronic *Mycobacterium tuberculosis* infection in mice. *J Immunol* 2002;**169**(6):3155–62.
2. Aderem A, Ulevitch RJ. Toll-like receptors in the induction of the innate immune response. *Nature* 2000;**406**(6797):782–7.
3. Akahoshi M, Nakashima H, Miyake K, Inoue Y, Shimizu S, Tanaka Y, et al. Influence of interleukin-12 receptor beta1 polymorphisms on tuberculosis. *Hum Genet* 2003;**112**(3):237–43.
4. Bashirova A, Markelov ML, Shlykova TV, Alibaeva RA, Frolova EI. The human RIL gene: mapping to human chromosome 5q31.1, genomic organization and alternative transcripts. *Gene* 1998;**210**(2):239–45.
5. Borm GF, den Heijer M, Zielhuis GA. Publication bias was not a good reason to discourage trials with low power. *J Clin Epidemiol*; 2008 [Epub ahead of print].
6. Carpenter S, O'Neill LA. How important are toll-like receptors for antimicrobial responses? *Cell Microbiol* 2007;**9**(8):1891–901.
7. Caylà JA, Plasència A, Galdós-Tanguis H, Jansà JM. Pulmonary tuberculosis in HIV-infected patients as criterion for AIDS in Europe. *Lancet* 1993; **342**(8862):50.
8. Chang JS, Huggett JF, Dheda K, Kim LU, Zumla A, Rook GA. *Mycobacterium tuberculosis* induces selective up-regulation of TLRs in the mononuclear leukocytes of patients with active pulmonary tuberculosis. *J Immunol* 2006;**176**(5):3010–8.
9. Fantuzzi G, Reed D, Qi M, Scully S, Dinarello CA, Senaldi G. Role of interferon regulatory factor-1 in the regulation of IL-18 production and activity. *Eur J Immunol* 2001;**31**(2):369–75.
10. Fraser DA, Bulat-Kardum L, Knezevic J, Babarovic P, Matakovic-Mileusnic N, Dellacasagrande J, et al. Interferon-gamma receptor-1 gene polymorphism in tuberculosis patients from Croatia. *Scand J Immunol* 2003;**57**(5):480–4.
11. Frieden TR, Sterling TR, Munsiff SS, Watt CJ, Dye C. Tuberculosis. *Lancet* 2003;**362**(9387):887–99.
12. Graham RR, Kozyrev SV, Baechler EC, Reddy MV, Plenge RM, Beuer JW, et al. A common haplotype of interferon regulatory factor 5 (IRF5) regulates splicing and expression and is associated with increased risk of systemic lupus erythematosus. *Nat Genet* 2006;**38**(5):550–5.
13. Gomez LM, Sanchez E, Ruiz-Narvaez EA, Lopez-Nevot MA, Araya JM, Martin J. Macrophage migration inhibitory factor gene influences the risk of developing tuberculosis in northwestern Colombian population. *Tissue Antigens* 2007;**70**(1):28–33.
14. Harada H, Takahashi E, Itoh S, Harada K, Hori TA, Taniguchi T. Structure and regulation of the human interferon regulatory factor 1 (IRF-1) and IRF-2 genes: implications for a gene network in the interferon system. *Mol Cell Biol* 1994;**14**(2):1500–9.
15. Janeway Jr CA, Medzhitov R. Innate immune recognition. *Annu Rev Immunol* 2002;**20**:197–216.
16. Janis EM, Kaufmann SH, Schwartz RH, Pardoll DM. Activation of gamma delta T cells in the primary immune response to *Mycobacterium tuberculosis*. *Science* 1989;**244**(4905):713–6.
17. Jouanguy E, Lamhamedi-Cherradi S, Altare F, Fondanèche MC, Tuerlinckx D, Blanche S, et al. Partial interferon-gamma receptor 1 deficiency in a child with tuberculoid bacillus Calmette–Guerin infection and a sibling with clinical tuberculosis. *J Clin Invest* 1997;**100**(11):2658–64.
18. Kamijo R, Harada H, Matsuyama T, Bosland M, Gerecitano J, Shapiro D, et al. Requirement for transcription factor IRF-1 in NO synthase induction in macrophages. *Science* 1994;**263**(5153):1612–5.
19. Kawasaki A, Kyogoku C, Ohashi J, Miyashita R, Hikami K, Kusaoi M, et al. Association of IRF5 polymorphisms with systemic lupus erythematosus in a Japanese population: support for a crucial role of intron 1 polymorphisms. *Arthritis Rheum* 2008;**58**(3):826–34.
20. Keller C, Hoffmann R, Lang R, Brandau S, Hermann C, Ehlers S. Genetically determined susceptibility to tuberculosis in mice causally involves accelerated and enhanced recruitment of granulocytes. *Infect Immun* 2006;**74**(7):4295–309.
21. Ko J, Gendron-Fitzpatrick A, Splitter GA. Susceptibility of IFN regulatory factor-1 and IFN consensus sequence binding protein-deficient mice to brucellosis. *J Immunol* 2002;**168**(5):2433–40.
22. Lohoff M, Ferrick D, Mittrucker HW, Duncan GS, Bischof S, Rollinghoff M, et al. Interferon regulatory factor-1 is required for a T helper 1 immune response in vivo. *Immunity* 1997;**6**(6):681–9.
23. Macaskill P, Walter SD, Irwig L. A comparison of methods to detect publication bias in meta-analysis. *Stat Med* 2001;**20**(4):641–54.
24. Negishi H, Fujita Y, Yanai H, Sakaguchi S, Ouyang X, Shinohara M, et al. Evidence for licensing of IFN-gamma-induced IFN regulatory factor 1 transcription factor by MyD88 in toll-like receptor-dependent gene induction program. *Proc Natl Acad Sci U S A* 2006;**103**(41):15136–41.
25. Newport MJ, Awomoyi AA, Blackwell JM. Polymorphism in the interferon-gamma receptor-1 gene and susceptibility to pulmonary tuberculosis in The Gambia. *Scand J Immunol* 2003;**58**(4):383–5.
26. Oddo M, Calandra T, Bucala R, Meyan PR. Macrophage migration inhibitory factor reduces the growth of virulent *Mycobacterium tuberculosis* in human macrophages. *Infect Immun* 2005;**73**(6):3783–6.
27. Ogasawara K, Hida S, Azimi N, Tagaya Y, Sato T, Yokochi-Fukuda T, et al. Requirement for IRF-1 in the microenvironment supporting development of natural killer cells. *Nature* 1998;**391**(6668):700–3.
28. Ohashi J, Yamamoto S, Tsuchiya N, Hatta Y, Komata T, Matsushita M, et al. Comparison of statistical power between 2 × 2 allele frequency and allele positivity tables in case-control studies of complex disease genes. *Ann Hum Genet* 2001;**65**:197–206.
29. Pan H, Yan BS, Rojas M, Shebzukhov YV, Zhou H, Kobzik L, et al. *Ipr1* gene mediates innate immunity to tuberculosis. *Nature* 2005;**434**(7034):767–72.
30. Pravica V, Asderakis A, Perrey C, Hajeer A, Sinnott PJ, Hutchinson IV. In vitro production of IFN-gamma correlates with CA repeat polymorphism in the human IFN-gamma gene. *Eur J Immunogenet* 1999;**26**(1):1–3.
31. Qiao Y, Prabhakar S, Coccia EM, Weiden M, Canova A, Giacomini E, et al. Host defense responses to infection by *Mycobacterium tuberculosis*. Induction of IRF-1 and a serine protease inhibitor. *J Biol Chem* 2002;**277**(25):22377–85.
32. Reiling N, Hölscher C, Fehrenbach A, Kröger S, Kirschning CJ, Goyert S, et al. Cutting edge: toll-like receptor (TLR)2- and TLR4-mediated pathogen recognition in resistance to airborne infection with *Mycobacterium tuberculosis*. *J Immunol* 2002;**169**(7):3480–4.
33. Remoli ME, Giacomini E, Lutfalla G, Dondi E, Orefici G, Battistini A, et al. Selective expression of type I IFN genes in human dendritic cells infected with *Mycobacterium tuberculosis*. *J Immunol* 2002;**169**(1):366–74.
34. Sahiratmadja E, Baak-Pablo R, de Visser AW, Alisjahbana B, Adnan I, van Crevel R, et al. Association of polymorphisms in IL-12/IFN-gamma pathway genes with susceptibility to pulmonary tuberculosis in Indonesia. *Tuberculosis (Edinb)* 2007;**87**(4):303–11.
35. Saito H, Tada S, Wakabayashi K, Nakamoto N, Takahashi M, Nakamura M, et al. The detection of IRF-1 promoter polymorphisms and their possible contribution to T helper 1 response in chronic hepatitis C. *J Interferon Cytokine Res* 2002;**22**(6):693–700.
36. Sato M, Taniguchi T, Tanaka N. The interferon system and interferon regulatory factor transcription factors - studies from gene knockout mice. *Cytokine Growth Factor Rev* 2001;**12**(2–3):133–42.
37. Sigurdsson S, Nordmark G, Go ring HHH, Lindroos K, Wiman A, Sturfelt G, et al. Polymorphisms in the tyrosine kinase 2 and interferon regulatory factor 5 genes are associated with systemic lupus erythematosus. *Am J Hum Genet* 2005;**76**:528–37.
38. Sims SH, Cha Y, Romine MF, Gao PQ, Gottlieb K, Deisseroth AB. A novel interferon-inducible domain: structural and functional analysis of the human interferon regulatory factor 1 gene promoter. *Mol Cell Biol* 1993;**13**(1):690–702.
39. Taki S, Sato T, Ogasawara K, Fukuda T, Sato M, Hida S, et al. Multistage regulation of Th1-type immune responses by the transcription factor IRF-1. *Immunity* 1997;**6**(6):673–9.
40. Taniguchi T, Harada H, Lamphier M. Regulation of the interferon system and cell growth by the IRF transcription factors. *J Cancer Res Clin Oncol* 1995;**121**(9–10):516–20.
41. Taniguchi T, Ogasawara K, Takaoka A, Tanaka N. IRF family of transcription factors as regulators of host defense. *Annu Rev Immunol* 2001;**19**:623–55.
42. Tosh K, Campbell SJ, Fielding K, Sillah J, Bah B, Gustafson P, et al. Variants in the SP110 gene are associated with genetic susceptibility to tuberculosis in West Africa. *Proc Natl Acad Sci U S A* 2006;**103**(27):10364–8.
43. Trinchieri G. Interleukin-12 and the regulation of innate resistance and adaptive immunity. *Nat Rev Immunol* 2003;**3**(2):133–46.
44. Tso HW, Ip WK, Chong WP, Tam CM, Chiang AK, Lau YL. Association of interferon gamma and interleukin 10 genes with tuberculosis in Hong Kong Chinese. *Genes Immun* 2005;**6**(4):358–63.
45. Tufariello JM, Chan J, Flynn JL. Latent tuberculosis: mechanisms of host and bacillus that contribute to persistent infection. *Lancet Infect Dis* 2003;**3**(9): 578–90.
46. van de Vosse E, Hoeve MA, Ottenhoff TH. Human genetics of intracellular infectious diseases: molecular and cellular immunity against mycobacteria and salmonellae. *Lancet Infect Dis* 2004;**4**(12):739–49.
47. Watanabe N, Taniguchi T. Involvement of positive (IRF-1) and negative (IRF-2) transcription factors in the gene regulation of the type I interferon system. *Tanpakushitsu Kakusan Koso* 1992;**37**(Suppl. 14):2813–22.
48. Williams BG, Dye C. Antiretroviral drugs for tuberculosis control in the era of HIV/AIDS. *Science* 2003;**301**(5639):1535–7.
49. World Health Organization. The World Health Report 2004—changing history; 2004.

Genes and Immunity (2009) 10, 77–83

www.nature.com/gene

ORIGINAL ARTICLE

Genome-wide SNP-based linkage analysis of tuberculosis in Thais

S Mahasirimongkol[1,2], H Yanai[2,3], N Nishida[4], C Ridruechai[5], I Matsushita[6], J Ohashi[4], S Summanapan[7], N Yamada[2], S Moolphate[2], C Chuchotaworn[8], A Chaiprasert[9], W Manosuthi[10], P Kantipong[11], S Kanitwittaya[12], T Sura[13], S Khusmith[5], K Tokunaga[4], P Sawanpanyalert[1] and N Keicho[6]

[1]*Medical Genetic Section, National Institute of Health, Department of Medical Sciences, Ministry of Public Health, Nonthaburi, Thailand;* [2]*TB/HIV Research Project, Research Institute of Tuberculosis, Japan Anti-Tuberculosis Association, Chiang Rai, Thailand;* [3]*Center for Collaborative Research and Institute of Tropical Medicine, Nagasaki University, Nagasaki, Japan;* [4]*Department of Human Genetics, Graduate School of Medicine, University of Tokyo, Bunkyo-ku, Tokyo, Japan;* [5]*Department of Microbiology and Immunology, Faculty of Tropical Medicine, Mahidol University, Bangkok, Thailand;* [6]*Department of Respiratory Diseases, Research Institute, International Medical Center of Japan, Shinjuku-ku, Tokyo, Japan;* [7]*Chiang Rai Provincial Health Office, Ministry of Public Health, Chiang Rai, Thailand;* [8]*Chest Disease Institute, Department of Medical Services, Ministry of Public Health, Nonthaburi, Thailand;* [9]*Department of Microbiology, Faculty of Medicine Siriraj Hospital, Mahidol University, Bangkok, Thailand;* [10]*Bamrasnaradura Infectious Diseases Institute, Ministry of Public Health, Nonthaburi, Thailand;* [11]*Chiang Rai Regional Hospital, Ministry of Public Health, Chiang Rai, Thailand;* [12]*Chiang Rai Regional Medical Sciences Center, Department of Medical Sciences, Ministry of Public Health, Chiang Rai, Thailand and* [13]*Department of Medicine, Faculty of Medicine Ramathibodi Hospital, Mahidol University, Bangkok, Thailand*

Tuberculosis, a potentially fatal infectious disease, affects millions of individuals annually worldwide. Human protective immunity that contains tuberculosis after infection has not been clearly defined. To gain insight into host genetic factors, nonparametric linkage analysis was performed using high-throughput microarray-based single nucleotide polymorphism (SNP) genotyping platform, a GeneChip array comprised 59 860 bi-allelic markers, in 93 Thai families with multiple siblings, 195 individuals affected with tuberculosis. Genotyping revealed a region on chromosome 5q showing suggestive evidence of linkage with tuberculosis (Z(lr) statistics = 3.01, logarithm of odds (LOD) score = 2.29, empirical P-value = 0.0005), and two candidate regions on chromosomes 17p and 20p by an ordered subset analysis using minimum age at onset of tuberculosis as the covariate (maximum LOD score = 2.57 and 3.33, permutation P-value = 0.0187 and 0.0183, respectively). These results imply a new evidence of genetic risk factors for tuberculosis in the Asian population. The significance of these ordered subset results supports a clinicopathological concept that immunological impairment in the disease differs between young and old tuberculosis patients. The linkage information from a specific ethnicity may provide unique candidate regions for the identification of the susceptibility genes and further help elucidate the immunopathogenesis of tuberculosis.
Genes and Immunity (2009) **10,** 77–83; doi:10.1038/gene.2008.81; published online 9 October 2008

Keywords: *linkage analysis; tuberculosis; Thais; 5q; 17p; 20p*

Introduction

Tuberculosis remains a serious public health problem in the developing world, especially in view of recent outbreaks of virtually untreatable, extensive drug-resistant tuberculosis.[1] A majority of individuals in endemic areas are infected with the pathogen *Mycobacterium tuberculosis* when they reach adulthood. In 2005, around 5 million individuals were diagnosed as having tuberculosis according to a WHO surveillance report.[2]

Correspondence: Dr N Keicho, Department of Respiratory Diseases, Research Institute, International Medical Center of Japan, 1-21-1, Toyama, Shinjuku-ku, Tokyo 162-8655, Japan.
E-mail: nkeicho-tky@umin.ac.jp
Received 30 June 2008; revised 11 August 2008; accepted 27 August 2008; published online 9 October 2008

Approximately 10% of those who are infected develop tuberculosis in their lifetime. Clinically and epidemiologically, three patterns of disease development after infection are often assumed, depending on the age at onset of tuberculosis and the prevalence of tuberculosis infection: (1) primary tuberculosis in adolescence; (2) reactivation of disease after infection and (3) exogenous re-infection in adulthood.[3] Primary tuberculosis is a disease that develops within the first few years after infection, often because of impaired host immunity, whereas reactivation of disease occurs later in life, after a long period of immune protection against development of the disease in infected individuals, together with the possibility of exogenous re-infection. Identification of a high-risk group corroborated by a specific mechanism for disease development would be one of the most desirable measures for controlling this disease in developing

countries, in which use of chemoprophylaxis for all infected individuals is an unacceptable burden on national tuberculosis control programs.

Contribution of host genetic factors to the development of this infectious disease has been classically observed. Until Koch[4] discovered the tubercle bacilli as the causative agent of tuberculosis, familial aggregation resulted in the initial perception that tuberculosis was a hereditary disease in the 19th century. An early study showed that monozygotic twins have higher risks of tuberculosis than dizygotic twins, given tuberculosis affected one of the twins.[5] Individual genetic variations in innate immunity, adaptive immunity and intracellular bacterial killing ability have roles in different phenotypes of tuberculosis. Disruption of genes in the *IL12/23–IFNG* pathway results in disseminated mycobacterial infection in susceptible infants.[6] Various association studies implicated this as one of the key pathways for containing tuberculosis.[7–9] Mutation in genes with ubiquitination functions have also been implicated as risks in both tuberculosis and leprosy.[10,11] On the basis of databases of genetic association study, nearly 100 genes had been studied for their association with tuberculosis. From these candidate gene association studies, apart from genes in *IL12/23–IFNG* axis, only *SLC11A1* (formerly *NRAMP1*) had been consistently shown evidence of association with tuberculosis.[12]

Prior to candidate gene approach, reverse genetic study in humans is often useful. Susceptibility genes based on novel disease regulatory mechanisms can be identified by hypothesis-free studies, such as genome-wide linkage and genome-wide association studies. In African populations, linkage analysis for tuberculosis earlier demonstrated suggestive evidence for linkage in two regions on chromosome 15 and chromosome X. Subsequent fine mapping of the chromosome 15 regions revealed *UBE3A* as a candidate susceptibility gene for tuberculosis.[10,13] Suggestive evidence of linkage was also found on chromosomes 10q26, 11q12 and 20p12 in the Brazilian population.[14,15] The only significant linkage evidence (logarithm of odds (LOD) = 3.49) to date is a study of 96 Moroccan multiplex families that implicated an autosomal-dominant gene on chromosome 8q12–q13.[16]

Distribution of virulent *M. tuberculosis* strains such as Beijing strain differs among regions of the world,[17] which suggests its adaptation to different human populations.[18] In the context of the host–pathogen relationship, human genetic studies in Asia may also reveal novel susceptibility/resistance genes in this field. In this study, linkage analysis in the Thai population was performed to gain insight into host genetic epidemiology of tuberculosis in Asians.

Results

Description of studied families

The numbers of families with multiple siblings affected with tuberculosis are shown in Table 1. Because of limited genotyping resources, only affected siblings were genotyped, which provided better linkage evidence when compared with genotyping the unaffected individuals in these families.

Table 1 Number of families and sibling pairs in the linkage analysis

	Number of families
Two affected siblings	87
Three affected siblings	5
Four affected siblings	0
Five affected siblings	1
Total families	93
Total number of independent sibling pairs (number of affected siblings-1, per family)	101

A total of 199 individuals from 95 families were originally genotyped using the *Xba*I 50 K microarray system, which is part of the 100 K affymetrix genotyping system. In the relationship analysis of the GRR program, ambiguous relationships were clarified and corrections were made before linkage analysis. Two of the 95 families (four individuals) were excluded because the analysis revealed that the affected individuals were half-siblings on the basis of their genotypes.

A stringent genotype call strategy was used to reduce the number of genotyping errors; criteria for genotype calling were more stringent than the standard criteria proposed by the manufacturer. The average call rate (percentage of successful genotype calls among subjects) was 98.08%. By using more stringent call criteria, the final call rate was 99.48%.

Linkage analysis

Linkage analysis was carried out with MERLIN; analysis without linkage disequilibrium (LD) correction showed inflation of the linkage statistics and noisy linkage spike patterns throughout the genome. LD was taken into account for the analysis by using LD patterns described earlier and MERLIN, which implements a method accounting for LD by inferred haplotypes from single nucleotide polymorphisms (SNPs) that showed LD with each other and used the inferred haplotypes as multi-allelic markers for linkage analysis.

After LD correction, a maximum LOD score of 2.29 was observed on chromosome 5q23.2–31.3 at 138.3 cM, with the LOD-1 support interval between rs1515641 (SNP_A-1673674, 131.9086, 127.2 Mb) and rs252101 (SNP_A-1739565, 141.01 cM, 141.3 Mb) (Table 2 and Supporting information Figures 2a and b). Simulation tests showed this linkage to be genome-wide suggestive evidence of linkage (0.25 peaks per genome scan). Regions that showed LOD score >1 were located on chromosomes 4, 5, 6, 11 and 14 (Table 2). All of these regions could be good candidates for follow-up positional study.

Age at onset analysis

Ordered subset analysis was used to determine whether the evidence for linkage differs according to age at onset. The results at which LOD scores reached the uncorrected significance value (*P*-value <0.05) are shown (Table 3). Two regions on chromosome 17p13.3–13.1 and chromosome 20p13–12.3 showed significantly higher LOD

Table 2 Chromosome regions with a non parametric LOD score with nominal significance ($P<0.01$)

Chromosome	*Peak SNP*	*Position (cM)*	*Physical position*	*LOD score*[a]	P-*value*
5q23.2–31.3	rs7706155	138.37	135 987 344	2.29	0.0005
	rs9327759	138.39	136 004 959		
	rs2188468	138.42	136 026 947		
11p15	rs1487214	29.85	19 588 715	1.62	0.003
14q32	rs8014257	109.60	98 321 756	1.48	0.005
6p12	rs10484980	78.13	54 559 585	1.33	0.007
4q26	rs2010003	121.27	118 807 065	1.3	0.007

Abbreviation: LOD, logarithm of odds.
[a]Calculated using the Kong and Cox linear model.

Table 3 Ordered subset analysis by minimum age at onset of tuberculosis in the families

Chromosome	*cM*	*Marker*	*No. of families in subset*	*Average age at onset (range)*	*Maximum LOD and (baseline LOD)*	P-*value*
17p13.3–13.1	13.5–13.7	rs2716912 rs10491086	32	19.47 (12–24) years	2.57 (0.14)	0.0187
20p13–12.3	10.6	rs750702	30	19.17 (12–23) years	3.33 (0.64)	0.0183

Abbreviation: LOD, logarithm of odds.

scores (permutation *P*-value at 0.0187 and 0.0183, respectively) (Figures 1a and b).

Discussion

In this study involving 93 Thai families (195 affected individuals), a region on chromosome 5q23.2–31.3 was shown to be a candidate region for tuberculosis susceptibility with suggestive evidence of linkage by genome-wide linkage analysis. From the ordered subset analysis, two regions on chromosome 17p13.3–13.1 and chromosome 20p13–12.3 were shown to have significant linkage with earlier onset of tuberculosis.

In the 5q candidate region, various genes, including a cluster of cytokine genes, *GM-CSF, IL3, IL4, IL5* and *IL13*, have been mapped. *IRF1*, a responsive element in the interferon-γ-mediated pathway, an antimicrobial peptide gene (*LEAP2*), and genes with ubiquitination activities, such as *APBB3* and *SPK1A*, have also been located. This chromosomal region has also been implicated in linkage analyses of the parasitic load of *Schistosoma mansoni*[19] and *Plasmodium falciparum*.[20] In addition, this region on chromosome 5 coincides with the *IBD5* region that showed significant evidence of linkage and association with Crohn's disease, an inflammatory bowel disease closely associated with *Mycobacterium paratuberculosis*.[21] It is interesting to note that the *IBD5* haplotype is distributed differently in Asian and European populations, and that the *IBD5* risk haplotype in Europeans is very rare in Asians.[22] Although candidate genes including *IL4*[23] and *CD14*[24,25] have been studied in this particular region, roles of these genes in tuberculosis remain inconclusive. Small sample size and ethnicity of the study populations may partially explain these equivocal association results. With this linkage evidence, polymorphisms within these genes should be the subjects for further validation in another Asian population.

From the functional viewpoint, this region has been reported to control the differentiation of Th2 lymphocytes, resulting in different levels of interleukin-4 (IL-4) and IL-5 from $CD4^+$ T-cell clones after exposure to parasite antigens, but not to affect the level of interferon-γ.[26] The predilection of this balance for Th2 may also play a role in susceptibility to tuberculosis. The predominant Th2 may partly influence tuberculosis susceptibility by the IL-4 and IL-13 capability of inhibiting autophagy by mycobacterium-infected macrophages.[27] IL-4 has been suggested to be a regulator of the immune response to tuberculosis antigen but not the disease *per se* in Brazilian families with multiple cases of tuberculosis.[23] This study suggests that the Th2 regulatory function of this region may play a more important role in tuberculosis susceptibility in the Thai population than in the Brazilian population. This genetic heterogeneity may reflect the host–pathogen interaction with specific mycobacterium strains: in Thailand, at least 20% of circulating strains are Beijing strains of Asian origin.[28] These virulent strains have been shown to preferentially stimulate Th2 response more than other non-virulent strains.[29]

From the ordered subset analysis of earlier onset of tuberculosis, the maximum linkage statistics (LOD = 3.33) on chromosome 20p were derived from 30 of the 93 families, and the average minimum age at onset of tuberculosis in these families was 19.17 years. The 20p region is of particular interest for tuberculosis susceptibility because it has been shown to have significant evidence of linkage with leprosy.[15,30] The susceptibility gene(s) in this region may play a role in susceptibility to primary tuberculosis in pediatric and adolescent cases. Several promising candidate genes in this region are a cluster of β-defensin genes that play important roles in innate immunity against respiratory infection.[31,32] The suggestive evidence of linkage for the region on chromosome 17p was derived from 32 families with the youngest age at onset, but with a lower maximum LOD score than for the 20p region. Although it is speculative at this stage, a possible candidate in the 17p13.3–13.1 region, *MYBBP1A* was recently identified as

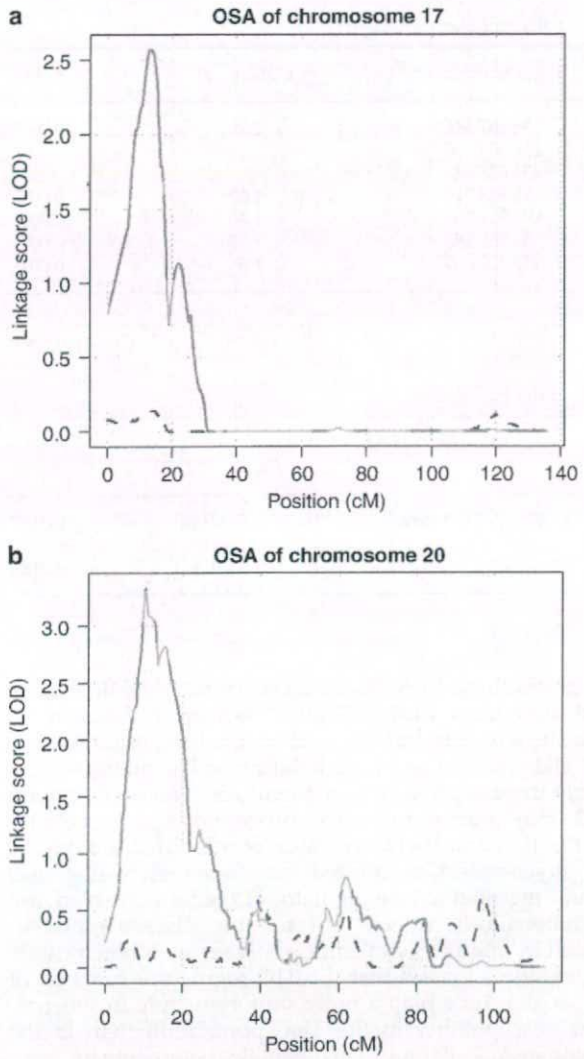

Figure 1 Ordered subset analysis (OSA) results on chromosome 17 and chromosome 20. The solid lines indicate the linkage statistics from the subset of families with younger age at onset. Thirty-two families and 30 families were grouped into the younger age at onset family for chromosome 17 (**a**) and chromosome 20 (**b**) respectively. The dotted lines indicate the statistics when all families were included in the analysis. (Image file = Fig1(a)_OSAChr17_black.pdf) (Image file = Fig1(b)_OSAChr20_black.pdf).

a co-repressor of NF-κB.[33] Although these two chromosome regions provide statistical evidence of possible linkage in subsets of these families, small number of families in the ordered subset analysis requires further confirmatory evidence either through additional linkage analysis or association study.

As for the regions on chromosomes 8, 15 and X reported in African populations, we could not find any evidence of linkage. Discordance of the results may be partially explained by the genetic heterogeneity in tuberculosis susceptibility in different human populations, and also by the differences in the distribution of *M. tuberculosis* strains.[18] We could improve the linkage evidence by genotyping more parental samples, but this may not be realistic given the small number of families in whom the parents are alive and available for enrollment. Confirmation of the linkage in another study with a larger sample size with extended genotyping of Asian families with tuberculosis and fine mapping around these candidate regions would be necessary to reinforce our findings in the future. A genome-wide association study provides an alternative tool for selective re-genotyping of the linkage regions and also is capable of revealing common low risk alleles even below the detection limit of linkage analysis. These hypothesis-free, reverse genetic approaches would elucidate the pathogenic mechanism and might enable effective treatment and prevention strategies for tuberculosis in the future.

Materials and methods

Ascertainment and collection of families

Families were ascertained mainly through a tuberculosis surveillance system in Chiang Rai province, the northernmost province of Thailand. Additional families were also recruited through the Central Chest Hospital in Bangkok, Thailand. In total, 95 families with at least two siblings affected with tuberculosis were ascertained. These families included 199 individuals affected with tuberculosis. A parent in a sibling pair family was genotyped because this parent was also affected with tuberculosis. Tuberculosis was diagnosed by clinical characteristics and microbiological confirmation by sputum culture or at least two out of three positive sputum smears. In a minority of cases, the diagnosis was obtained from earlier records in the tuberculosis surveillance system supplemented by an abnormal current chest X-ray. This study was reviewed and approved by The Ethical Review Committee for Research in Human Subjects (Ministry of Public Health, Thailand) and the Institutional Review Board of the International Medical Center of Japan. The patients were tested for HIV using the standard serological test, and HIV-infected patients were not included in this study. Venous blood samples were collected from the patients after individual informed consent was obtained by our field researchers.

Genotyping

Genomic DNA extraction from blood samples was performed using the QIAamp blood midi kit (Qiagen, Hilden, Germany) and quantification was performed using a nanodrop spectrometer to a concentration of 50 ng μl^{-1}. The *Xba*I microarray chip of the mapping 100 K Array (Affymetrix, Santa Clara, CA, USA) was used for genotyping, following the standard genotyping protocol for the GeneChip Mapping 100 K Array. In summary, 5 μl of 50 ng μl^{-1} (250 ng) of genomic DNA were digested with the restriction endonuclease (*Xba*I) and ligated to adaptors with the T4 ligase that recognizes the cohesive four base-pair overhangs. A generic primer that recognizes the adaptor sequence was used to amplify adaptor-ligated DNA fragments. Preferential amplification of fragments in the 250–2000 bp size range was performed by the optimized PCR conditions. The amplified DNA was purified by the DNA amplification clean-up kit (Takara Bio, Shiga, Japan) and then fragmented, labeled and hybridized to the *Xba*I chip of the mapping 100 K set.

Genotype calling algorithm and quality control
Genotype calls for each chip were given by the BRLMM algorithm using a confidence call threshold of 0.3. The BRLMM algorithm is based on modification of the RLMM algorithm, which showed a call accuracy superior to that of the dynamic modeling algorithm.[34] The confidence call threshold was set at a lower threshold than the standard call threshold (0.5) to select only SNPs with higher call confidence and to reduce the effect of genotyping errors in linkage analysis. SNPs with missing rates of more than 5% were excluded from the later analysis. Thus, the average genotype call rate was 99.48% for 52 433 SNPs selected from 58 960 SNPs on the *Xba*I chip.

Quality control and Mendelian error checking
ALOHOROMA was used for quality control and preparation of input files and semi-automated linkage analysis using the Perl script.[35] The gender of each sample was checked with the number of heterozygosities at SNPs on chromosome X, and there was complete concordance between the reported sex and the genotyped sex. PedCheck was used for exclusion of markers that were in Mendelian inconsistence, and 339 genotypes data were deleted.[36]

Markers with significant deviation from Hardy–Weinberg's equilibrium (P-value <0.01) were filtered before the downstream analysis. The relatedness of these samples was analyzed using the GRR program, which analyzed the pair-wise relatedness for each pair of samples in the data set.[37] Mendelian error checking was also performed using MERLIN, with the error automatically wiped out before linkage analysis.[38] The map order and distances between SNP markers were based on the information provided by the manufacturer, with the flanking sequences of each of the SNPs aligned with the May 2004 release of the human genome sequence. LD patterns of these SNPs were determined using Haploview version 3.2. Because the tagging SNP selection algorithm had not been implemented for chromosome X in HAPLOVIEW V 3.2, we used the haplotype inference information based on a spine of strong LD ($D'>0.8$) for correction of LD in X chromosome analysis.[39] LD parameters were calculated by Haploview for every pair of markers situated within 1 Mb from each other. The LD information was used for the selection of tagSNPs to reduce the effect of LD on linkage statistics. TagSNPs were selected using a pairwise tagging strategy with $r^2>0.4$ as the threshold for the selection of independent markers. These tagSNPs in autosomal chromosomes and haplotype inferences in chromosome X were later used in linkage analysis by MERLIN. The final set of markers used for later analysis included 33 365 markers selected as the tagging set ($r^2<0.4$) from all available markers.

Linkage analysis
Nonparametric multipoint linkage analysis was carried out by MERLIN using all markers that passed the quality control criteria. LD was accounted for in the analysis by reanalyzing the data using haplotype block information derived from HAPLOVIEW (spine of strong LD, $D'>0.8$) on chromosome X and reanalyzing by using only tagSNPs ($r^2>0.4$ in the 1 MB region) in autosomal regions to reduce the effect of LD on linkage analysis. Population allele frequencies of these SNPs were inferred from unrelated individuals in the samples by MERLIN.

MERLIN recently provided a method to account for LD by determining the haplotype of SNPs in strong LD and using inferred haplotypes as multiallelic markers.[40] Effects of LD on the linkage analysis were investigated by comparison of nonparametric linkage statistics with and without haplotype block information and tagSNPs for linkage analysis (Supporting information Figure 2a and b). The significant levels of linkage statistics were assessed by 10 000 gene dropping simulation. The simulation was carried out with data from chromosome 22 to reduce the computation time. The numbers for each of the linkage statistics from the simulations were multiplied by 44 to compensate for the expected size of the whole genome compared with chromosome 22. The suggestive and significant evidences of linkage by this simulation were observed at LOD score levels of 1.79 and 3.12, respectively.

Ordered subset analysis with age at onset
Age at onset was taken into account for linkage analysis using the age at diagnosis of tuberculosis. When the age at diagnosis was not available, the patient's current age was imputed to replace the age at diagnosis. Only nine data points were imputed using the current age at ascertainment. Our ascertainment scheme only identified patients who developed tuberculosis within the past 10 years, and the current age at ascertainment should be fairly accurate for imputation. The age at onset was analyzed as a covariate using ordered subset analysis by the FLOSS program.[41] The minimum age at onset of tuberculosis was used as the covariate because it is more likely that tuberculosis occurred at a younger age caused by immunological impairment to tuberculosis rather than by repetitive external mycobacterium exposures or endogenous immune senescence when compared with tuberculosis in the elderly population. FLOSS accepts the MERLIN LOD score outputs per family for reanalyzing the linkage statistics by ordering the families by the supplied covariate. The linkage analysis was re-performed by adding one family at a time, and the highest linkage score from the ordered subset analysis was chosen as the plausible linkage when age at onset presented in the disease model. The significance of the ordered subset analysis was calculated by simulation through re-sampling of equal numbers of families that provided the maximum linkage statistics from all available families, and then the number of times the re-sampling statistics exceeded the highest observed statistics was counted. The significant levels of the ordered subset analysis can be considered chromosome-wide with a permutation P-value <0.025 and genome-wide significant with a permutation P-value <0.001. This analysis technique is robust against heterogeneity and should be useful in analysis of linkage in tuberculosis that showed two peaks of higher incidence in two different age groups, that is young adult and elderly populations.

Acknowledgements

This study was partly supported by International Cooperation Research Grant, the Ministry of Health,